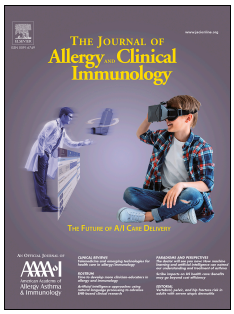
Journal Pre-proof



Single Cell Transcriptomic Analysis Reveals Key Immune Cell Phenotypes in the lung of Asthma Exacerbation

Hui Li, MMED, Huaqi Wang, PhD, Leon Sokulsky, PhD, Shaoxia Liu, PhD, Rui Yang, PhD, Xiaojie Liu, BMED, Lujia Zhou, BMED, Juan Li, PhD, Chun Huang, MMED, Fangfang Li, MMED, Xu Lei, MMED, Hongxia Jia, MMED, Jiuling Cheng, MMED, Fuguang Li, PhD, Ming Yang, PhD, Guojun Zhang, PhD

PII: S0091-6749(20)31400-7

DOI: https://doi.org/10.1016/j.jaci.2020.09.032

Reference: YMAI 14780

To appear in: *Journal of Allergy and Clinical Immunology*

Received Date: 5 April 2020

Revised Date: 2 September 2020

Accepted Date: 11 September 2020

Please cite this article as: Li H, Wang H, Sokulsky L, Liu S, Yang R, Liu X, Zhou L, Li J, Huang C, Li F, Lei X, Jia H, Cheng J, Li F, Yang M, Zhang G, Single Cell Transcriptomic Analysis Reveals Key Immune Cell Phenotypes in the lung of Asthma Exacerbation, *Journal of Allergy and Clinical Immunology* (2020), doi: https://doi.org/10.1016/j.jaci.2020.09.032.

This is a PDF file of an article that has undergone enhancements after acceptance, such as the addition of a cover page and metadata, and formatting for readability, but it is not yet the definitive version of record. This version will undergo additional copyediting, typesetting and review before it is published in its final form, but we are providing this version to give early visibility of the article. Please note that, during the production process, errors may be discovered which could affect the content, and all legal disclaimers that apply to the journal pertain.

© 2020 Published by Elsevier Inc. on behalf of the American Academy of Allergy, Asthma & Immunology.

Journal Pre-proof

Single Cell Transcriptomic Analysis Reveals Key Immune Cell Phenotypes in the lung of Asthma Exacerbation

Hui Li, MMED[1, †], Huaqi Wang, PhD[1, †], Leon Sokulsky, PhD[2], Shaoxia Liu, PhD[1], Rui Yang, PhD[1], Xiaojie Liu, BMED[3], Lujia Zhou, BMED[3], Juan Li, PhD[1], Chun Huang, MMED[1], Fangfang Li, MMED[1], Xu Lei, MMED[1], Hongxia Jia, MMED[1], Jiuling Cheng, MMED[1], Fuguang Li, PhD[3], Ming Yang, PhD[2, 3] * and Guojun Zhang, PhD[1, *]

[1]Department of Respiratory Medicine, The First Affiliated Hospital of Zhengzhou University, No.1, Jianshe East Road, Zhengzhou, Henan 450052, P.R. China.

[2]Priority Research Centre for Healthy Lungs, School of Biomedical Sciences & Pharmacy, Faculty of Health and Hunter Medical Research Institute, University of Newcastle, Callaghan, NSW 2300, Australia

[3]Academy of Medical Sciences & Department of Immunology, College of Basic Medical Sciences, Zhengzhou University, Zhengzhou, Henan 450052, China

[†] Hui Li and Huaqi Wang contributed equally. * Ming Yang and Guojun Zhang contributed equally.

Corresponding Author Information: Guojun Zhang, Department of Respiratory Medicine, The First Affiliated Hospital of Zhengzhou University, No.1, Jianshe East Road, Zhengzhou, Henan 450052, P.R. China and Ming Yang, Academy of Medical Sciences, Zhengzhou University & Priority Research Centre for Healthy Lungs, School of Biomedical Sciences & Pharmacy, Faculty of Health & Hunter Medical Research Institute, Lot 1 Kookaburra Circuit,

Journal Pre-proof

Journal Pre-proof

New Lambton Heights, NSW 2305, Australia. Email Address: gjzhangzzu@126.com (G.J.Z) or ming.yang@newcastle.edu.au (M.Y)

Disclosure statement

The authors declare no conflict of interest.

Word Count: 6379 (including abstract)

Journal Pre-proof

Journal Pre-proof

ABSTRACT

Background: Asthma exacerbations are associated with heightened asthma symptoms, which can result in hospitalization in severe cases. However, the molecular immunological processes that determine the course of an exacerbation remains poorly understood, impeding the progression of developing effective therapies.

Objective: To identify candidate genes that are strongly associated with asthma exacerbation at a cellular level.

Methods: Asthmatic and healthy control subjects were recruited, and bronchoalveolar lavage fluid (BALF) was isolated from these subjects via bronchoscopy. Cells were isolated through FACS, and single-cell RNA sequencing was performed on enriched cell populations.

Results: We show that the levels of monocyte, $CD8^+$ T cells, and macrophages are significantly elevated in the BALF of patients. A set of cytokines and intracellular transduction regulators are associated with asthma exacerbations and are shared across multiple cell clusters, forming a complicated molecular framework. An additional group of core exacerbation-associated modules is activated, including EIF2 signaling, Ephrin receptor signaling, and CXCR4 signaling in the subpopulations of $CD8^+$ T cells (C1-a) and monocytes (C7) clusters, which are associated with infection.

Conclusion: Our study identifies a significant number of severe asthma-associated genes that are differentially expressed by multiple cell clusters

Clinical Implications: Our study provides an insightful framework to explore, in a clinical setting, the pathogenesis of the disease and identifies therapeutic targets that should be further explored in exacerbation treatments.

Journal Pre-proof

Capsule Summary

This study provides a comprehensive analysis of individual immune cell population, isolated from the bronchoalveolar lavage fluid of asthmatics and healthy controls, that have undergone RNA-sequencing.

Key Words

Asthma, Single Cell RNA-sequencing, T-lymphocytes, B-lymphocytes, Monocytes, Neutrophils, Macrophages, Cytokines, Chemokines

Abbreviations

AHR-Airways Hyperresponsiveness

Th-T-helper cell

ILC2-Innate Lymphoid cell type 2

NK-Natural Killer Cell

scRNA seq-Single Cell RNA sequencing

BALF-Bronchoalveolar Lavage Fluid

FACS-Fluorescent Activated Cell Sorting

CD-Cluster Differentiation

UMIs-Unique Molecular Identifiers

IFN-Interferon

IgE-Immunoglobulin E

IL-Interleukin

Journal Pre-proof

Journal Pre-proof

INTRODUCTION

Patients with asthma exacerbations typically present with exaggerated inflammation, mucus hypersecretion in the airways, and airways hyperresponsiveness (AHR), and require hospitalization if mainstay therapies are ineffective. A wide range of common factors contributes to increased susceptibility to asthma exacerbation, including allergen, respiratory infection, cigarette smoke, and air pollutants (1). The etiology of asthma exacerbations is heterogeneous, which results from a complex network of innate and adaptive host defense responses (2). It remains unclear about the diverse molecular network underpinning the aberrant immune responses in the lung during exacerbation. Current treatments, including glucocorticoids and β2 agonists that are effective for stable disease, have limited effects on controlling symptoms in patients with asthma exacerbations (3), and the lack of targeted therapies for the treatment of exacerbation remains a significant unmet clinical need and requires mechanistic investigations to identify future therapeutic approaches.

Eosinophil infiltration is believed to be a hallmark feature of allergen-induced exacerbation, which is predominantly regulated by type-2 immunity driven by $CD4^+$ T-helper 2 (Th2) cells and innate lymphoid cells (ILC2s) (4). However, some patients with type-2 high phenotype demonstrated persistent Th2 induced airway inflammation despite high doses of inhaled glucocorticoids that typically suppresses Th2 lymphocytes (5), and antibodies targeting type-2 cytokines and eosinophils decrease but do not extinguish exacerbations and clinical hallmark features of the disease (6-8). Several lines of evidence suggest that asthma exacerbations are linked to respiratory viral infection and Th1 or Th17 regulated immunity (9, 10). Other immune cells, including macrophages, neutrophils, and NK cells that associate with respiratory anti-viral immune responses, are implicated in the pathogenesis (11). In addition, multiple immune pathways that involve viral sensing and interferon production have also been associated with disease exacerbations (12). Therefore, the current investigation has

Journal Pre-proof

not comprehensively determined the interaction among numerous molecular pathways in each cell that may result in asthma exacerbations.

Recently, multiple large cluster studies, including the Severe Asthma Research Program (SARP), the Unbiased Biomarkers for the Prediction of Respiratory Disease Outcome (U-BIOPRED) and Airways Disease Endotyping for Personalized Therapeutics (ADEPT) attempted to obtain mechanistic insight into the molecular mechanisms of the diseases (13-15). These studies have demonstrated the complex inflammatory networks underlying the severity of the disease, leading to different treatment responses. Furthermore, other methods, including RNA transcriptomics analysis of bronchial tissue, blood and sputum, and metabolomics, have been employed to determine biomarkers for asthma severity and steroid resistance (14, 16-18). Despite the insight provided from these analyses, they were unable to discern between association and causation in the context of immune-pathways and the resultant asthma exacerbation. Network-based approaches are increasingly recognized as efficient tools to analyze high dimensional data of disease and to extract informative gene association in biomedical research in an attempt to counteract this issue. Systematic network investigation provides an unbiased mechanistic understanding of the pathogenesis of asthma exacerbations (19). However, previous multi-omics studies have not been designed to identify molecular networks specific to individual immune cells in asthma exacerbations either due to bulk tissue biopsies or a limited set of predefined markers being used. This limits our ability to interpret the basis for immune response underpinning the pathogenesis at the cellular level.

To address this issue, we employed a microfluidic-based system for high dimensional single-cell RNA deep sequencing (scRNA Seq) to profile RNA transcriptome of individual immune cells in Bronchoalveolar Lavage Fluid (BALF) of patients with asthma exacerbation. scRNA Seq has been developed recently to investigate the complex relationship between

Journal Pre-proof

heterogeneous cells and determine the transcriptome profile of vast genes at single-cell level (20). Recently, a study of mild or moderate asthma has detected pathogenic effector Th2 cells in lower airways, which play a key role in the abnormal state of the epithelial cells (21). Furthermore, a mouse model of house dust mite-induced allergic asthma has elegantly shown gene expression pattern of Th2 cells in an unbiased manner, suggesting their crucial roles in the disease (22). In this study, scRNA seq allows us to determine the pathophysiological changes of asthma exacerbation in the lung with unprecedented detail. We found the expression of 7092 genes to be differentially changed in 16 cell types. Our analyses revealed significantly increased heterogeneity of immune cells of both macrophage and monocyte lineages, in comparison to normal BALF. This heterogeneity was highlighted by combinatorial expression of genes reflecting responses to various environmental stimuli. The observed continuum of macrophage cell state argues strongly against the classical notion of a few discrete states of differentiation or activation shaping the lung microenvironment of asthma patients during exacerbations. This vast transcriptome data of immune cells can be used as a valuable resource for interrogating the essential characteristics of immune cells and for potentially guiding effective therapy strategies.

Journal Pre-proof

Journal Pre-proof

MATERIAL AND METHODS

Study design and eligibility

This study was designed to profile transcriptomic changes in single immune cells. Subjects studied included a cohort of asthmatic patients who were admitted to the hospital for a diagnosis of asthma exacerbation and a cohort of healthy subjects between February 2019 and June 2019, and the selection criteria was adapted as previously published (23, 24). Briefly, an individual was eligible for enrolment if: was 18 years of age; was diagnosed with asthma by a clinician more than one year before investigation; required emergency care and hospitalization due to worsening of the respiratory symptoms; was a nonsmoker; and signed the consent form, as per central institutional review board (IRB) guidelines. This study was approved by the Ethics Committee of Scientific Research and Clinical Trials of the First Affiliated Hospital of Zhengzhou University (#2019-KY-172).

Subjects were excluded if they were pregnant or breast-feeding; was receiving immunotherapy including anti-IgE therapy or had received immunotherapy in the previous 3 months; had clinically significant abnormalities on complete blood count; was treated with systemic corticosteroids for any medical condition including an asthma exacerbation within the previous 2 weeks; had a cold within the previous 7 d; was participating in an asthma-related pharmaceutical study or intervention study or had participated in such a study within the previous 4 weeks; required greater than 500 μg of fluticasone plus a long-acting beta-agonist delivered by one puff twice daily or its equivalent and/or used oral corticosteroids daily or every other day; had any medical illnesses that in the opinion of the investigators would increase the risk incurred by participating in the study, interfere with measured outcomes, or interfere with performance of study procedures; had concurrent medical problems that required systemic corticosteroids or other immunomodulators; was diagnosed

with cancer or had a history of cancer; was not able to perform pulmonary function tests; had known hypersensitivity to any medications used for asthma treatment;

Healthy subjects.

Nine healthy control subjects were recruited. All healthy control subjects had no history of pulmonary disease, allergic rhinitis, or any other atopic disease. In pulmonary function tests, all healthy control subjects had normal airway responses to inhaled methacholine and normal FEV1 (FEV1 percent predicted >80%). Four healthy control subjects were excluded for having evidence of positive test results for more than 5 common aeroallergens on ImmunoCAP immunologic testing.

Bronchoscopy Procedure

All subjects underwent fibreoptic bronchoscopy with lavage, as previously described (25). BALF samples were collected within 12 hours of their admission to the hospital before issuing medication. Symptoms of patients were closely monitored to ensure their safety when undergoing bronchoscopy. A 4.5-mm-diameter endotracheal tube was used to allow for the use of a 3.5-mm fiberoptic bronchoscope with lavage port while ensuring adequate airflow. Following the placement of peripheral intravenous access, all subjects were under continuous monitoring with pulse oximetry and cardiorespiratory for a total of four hours during and after the procedure. Lidocaine was used to anesthetize the vocal cords, and the bronchoscope was then passed into the trachea. Multiple aliquots of 2% lidocaine were used to spray the carina and right and left main stem bronchi. The fibreoptic bronchoscope was wedged into the right middle lobe bronchus under the direct inspection of all primary segments of main stem bronchi. Six aliquots of 20 ml prewarmed 37^{o}C sterile saline were instilled and immediately aspirated through the bronchoscope by immediate gentle hand suction. The aliquots were pooled together into a single sample and immediately placed on ice, with the

Journal Pre-proof

Journal Pre-proof

examination of total cell counts, FACS sorting, RNA extraction and single-cell deep-sequencing preceding collection.

FACS Sorting

After obtaining BALF samples, red blood cells were lysed and washed with ice-cold PBS. Cells were then counted with Trypan blue and stained with 7-AAD. BALF cells were stained with anti-human CD45. Live $CD45^+$ cells were collected on a FACSAria III flow cytometer (BD Biosciences).

Single-cell gene expression

To surrogate the transcriptomic profile of single immune cells in BALF, we used the BD Rhapsody Single-Cell Analysis System (BD Biosciences) as previously reported (26). Briefly, single-cell capture of sorted BALF $CD45^+$ cells was obtained by randomly distributing across >200,000 microwells. Beads with unique molecular identifiers (UMIs) were added to microwells to allow a single bead to pair with a single cell. Lysis buffer was used to lysis cells for RNA molecules to hybridize to the beads. Beads were harvested into a single tube to synthesis cDNA with reverse transcription. Individual cDNA molecule was then labeled on the 5′ end (that is, the 3′ end of an mRNA transcript) with a molecular index and cell label indicating its cell of origin. Second strand cDNA was synthesized, followed by ligation of the adaptor for universal amplification for Transcriptome libraries with BD Rhapsody single-cell whole-transcriptome amplification kit. Eighteen cycles of PCR were used to amplify the adaptor-ligated cDNA products.

To generate sequencing libraries, random priming PCR of the whole-transcriptome amplification products were used to enrich the 3′ end of the transcripts linked with the cell label and molecular indices. Sequencing libraries were measured by a High Sensitivity DNA chip (Agilent) on a Bioanalyzer 2100 and the Qubit High Sensitivity DNA assay (Thermo

Journal Pre-proof

Fisher Scientific). 1.5 pM of the library for each sample was loaded onto a NextSeq 500 system and sequenced using High Output sequencing kits (75× 2 bp) (Illumina).

The BD Rhapsody analysis pipeline was employed to examine sequencing data (.fastq files). Cell labels and molecular identifiers were detected, and the identity of the individual gene was established by alignment against the genecode comprehensive hg38 reference. A table containing molecule counts per gene per cell was the output. 6,067 and 6,927 cells were identified for healthy and asthma exacerbations groups, respectively, with an average number of reads of around 15,668, an average of about 5,378 molecules and approximately 2,094 number genes detected per cell with average molecular index coverage (i.e., the number of times a molecule was sequenced) of around 2. A total of 36,483 genes were detected across all cells. Cells with mitochondrial gene (with a gene symbol starting with MT) content >5%, were discarded. Pseudogenes were removed. tSNE projection of the data was performed using default parameters (26). To determine the set of genes contributing to the separation of cell clusters, differential gene expression analysis (DEseq) based on negative binomial distribution was conducted to compare gene expression profiles in cells in each cluster versus those in the rest of the dataset.

Bioinformatic analysis of scRNA Seq data

Gene expression matrix generated by the 10X Cell Ranger aggregate option was further analyzed with R package Seurat (version 3.0) with default parameters. The data were filtered based on the following thresholds: less than 200 or greater than 2500 as unique expressed genes (nFeature_RNA) and greater than 5% as the percentage of mitochondrial genome content. The data were then normalized by converting with a scale factor (default as 10,000) and log-transformed with Seurat embedded function. A correlation analysis was performed by employing the RunPCA function of the Seurat package, following by an integrated analysis of the three datasets. Clustering analysis was carried out with standard Seurat

Journal Pre-proof

package procedures, with a resolution at 1.2. The identified clusters were then visualized using t-distributed Stochastic Neighbour Embedding of the principal components (t-SNE) in Seurat.

Average gene expression matrices were then retrieved for each cluster, and differential expression among clusters was performed to identify the top markers at a higher level by each cluster, with FindAllMarkers implemented function (parameters: only.pos = FALSE, min.pct = 0.2, thresh.use = 0.2). Cell clusters were annotated with SingleR that identifies unbiased cell types recognition of scRNA-seq, by comparing to Immunological Genome Project (www.immgen.org). Spearman correlation analysis was performed on variable genes after comparing it with each sample in the reference dataset. The coefficient of multiple correlations (per cell type) was aggregated to provide a single value per cell type per single cell.

Function of AddModuleScore in Seurat was used to calculate supervised module scores of each single cell, based on the scoring strategy that was previously described (27). Briefly, the average expression levels of each cluster on a single cell level were calculated, subtracted by the aggregated expression of control feature sets. All analyzed features were binned based on averaged expression, and the control features were randomly selected from each bin. For some t-SNE plots, feature plots were demonstrated for selected marker genes using Seurat function FeaturePlot. Pathway enrichment analysis examining enriched processes in clusters was performed using Ingenuity Pathways Analysis (IPA) (28). The results of IPA analysis are provided in Table E1, E2 and E3.

Statistical analysis

Statistical analysis was performed using Prism version 6.0 (GraphPad Software, USA). Two-way ANOVA was used to identify differences between two or more experimental groups, and Student-unpaired t-tests were used where comparison was made between two treatment

Journal Pre-proof

groups. All results are presented as means ± SEM, and P values < 0.05 were considered statistically significant.

Journal Pre-proof

Journal Pre-proof

RESULTS

Characterization of the participants

We enrolled 16 adults, 11 patients with asthma exacerbations, and five healthy controls without asthma (Table 1). There were six women and five men in the participants with asthma exacerbations. Those patients had a mean age of 42.9 years, who had impaired lung function with a mean FEV1% predicted (SEM) of 85.76 (4.85). The Patients had significantly elevated total white blood cells with a mean (SEM) level of 7.313 (0.5688)$\times 10^9$/L, among which the levels neutrophil, eosinophil, monocytes, and lymphocytes were at 4.375(0.445) $\times 10^9$/L (0.445), 0.3909(0.1597) $\times 10^9$/L, 0.4791(0.03304) $\times 10^9$/L and 2.038(0.2052) $\times 10^9$/L, respectively. The serum IgE levels were at 358.5(155.6) IU/ml and the FENO levels at 56.82(14.6) ppb, which were significantly higher than those of healthy controls. Six patients with asthma exacerbation had greater than two exacerbations in the past year, with five of the eleven patients requiring hospitalization and two patients visiting ED. Healthy controls were aged between 31 to 62 years, with a mean age of 44.4 years. There were three females and two males.

scRNA-seq on lung immune cells identifies multiple clusters of immune cells

Single-cell RNA sequencing was generated from BALF samples from 11 patients with asthma exacerbations and 5 healthy subjects by using BD Rhapsody Single-Cell Analysis System (26). Single $CD45^+$ cells from BALF were purified by FACS AriaIII. Approximately 5378 molecules were detected per cell, and over 15,668 different genes were detected overall, with 2094 of them found to be differentially expressed. Outliers expressing <200 or >2,500 of nFeature_RNA were omitted from those groups, Doublets were also removed with Doublet-Finder (29). Principle component analysis (PCA) was performed on cells after normalization for the gene numbers detected in each group.

By analyzing the $CD45^+$ immune cells in BALF, we identified 69 distinct clusters with specific molecular markers by using SingleR, as shown by heatmap (Fig. 1 and E1). Each cell was defined to known immune cell types, including B cells, monocyte-derived DCs, alveolar macrophages, monocyte-derived macrophages, monocytes, neutrophils, NK cells, $CD4^+$ T cells, and $CD8^+$ T cells. Interestingly, we were able to detect a small proportion of bronchial epithelial cells, stem cells (HSC_$CD34^+$), and progenitor cells (CMP and GMP). The activation status of those cells was also identified.

Asthma exacerbations result in distinct cell clusters in BALF

After analyzing the aforementioned cell clusters, we further defined those cells into 16 major cell clusters (Fig. 2A). The level of five cell clusters was significantly elevated in the BALF of patients with asthma exacerbations, including Cluster (C) 6 (macrophage: monocyte−derived:IL−4/Dex/TGFβ) and 7 (monocyte: S-typhimurium-flagellum). The level of part of macrophage cluster (C0) and $CD8^+$ T cell (C1) clusters was also elevated (Fig. 2B).

To examine the expression of proinflammatory factors, we examined the cytokine profile of identified cell clusters (Fig. 2C). Cell clusters of healthy subjects did not produce significant levels of pro-inflammatory factors, except that CCL5 was by C1 ($CD8^+$ T cells) of both health and patients with asthma exacerbation. As for patients with asthma exacerbation, their C8 cluster (granulocyte-monocyte progenitor) was the predominant cellular source of IL-1A, whereas C0 (macrophage: alveolar), C1 ($CD8^+$ T cells), C3 (macrophage: monocyte derived:M−CSF/IFNγ), C4 (monocyte-derived macrophages), C6 (macrophage: monocyte−derived:IL−4/Dex/TGFβ), C9 (monocyte: anti-FcgRIIB), C12 (memory B cells), C13 (NK cells) and C14 (monocyte:$CD16^-$) expressed this cytokine to a lesser extent (Fig. 2C). Approximately 50% of neutrophils of patients with asthma exacerbation strongly expressed IL-1B. IL-18 was mildly expressed by a few cell clusters, including macrophage and monocyte clusters of patients with asthma exacerbations. IL-27 was mainly detected in

Journal Pre-proof

C3 (macrophage: monocyte−derived:M−CSF/IFNγ) and C9 (monocyte: anti-FcgRIIB). CCL2 and CCL5 were predominantly expressed by C1 ($CD8^+$ T cells) and C14 (monocytes:$CD16^-$), respectively. Interestingly, TSLP and CCL24 was dimly expressed C0 (macrophage: alveolar) and C15 (neutrophil). IFNγ and TNFα were broadly detected in $CD8^+$ T cells, NK cells, macrophage, and monocyte cell clusters. Interestingly, the GMP cluster expressed TNFα, and memory B cell generated IFNγ. Furthermore, GMP was active as these cells expressed a wide range of cytokines, including IL-1B, IL-6, and IL-18, albeit to a lesser extent. Additionally, we were also able to detect the expression of TGFβ1 and TGFβ2 in multiple cell clusters.

Intracellular signaling activity analyses

Intracellular transcriptional regulates importantly modulate pro-inflammatory responses of immune cells. After analyzing 32 critical transcriptional regulators, these factors were differentially expressed in the 16 cell clusters of asthma exacerbation patients, as compared to healthy controls (Fig. 3). C1 ($CD8^+$ T cells) cluster strongly expressed IKZF3, RELA, RNUX3, STAT4, STAT5A/5B, and TBX21 with relatively weaker expression of other transcriptional regulators. C3 (macrophage: monocyte−derived:M−CSF/IFNγ) cluster of asthma exacerbations strongly expressed SPI1 and STAT1 while those of healthy to a lesser extent. C12 (memory B cells), C13 (NK cells), and C14 (monocyte: $CD16^-$) clusters strongly and differentially expressed the majority of those regulators, while C15 (neutrophil) highly expressed BCL6, RUNX1 and RUNX3. By contrast, C2 (T_cell:$CD4^+$_effector_memory), C5 (T_cell: $CD4^+$_central_memory), C7 (monocyte: S_typhimurium_flagellin), C10 (monocyte: leukotriene_D4) and C11 (T_cell: gamma−delta) clusters only weakly expressed most of those transcriptional regulators. For healthy controls, most of these factors were not expressed except BCL6 of C15 (neutrophil), SPI1, and STAT1 of C0 (macrophages: alveolar), C3 (macrophage: monocyte−derived:M−CSF/IFNγ), and C9 (monocyte: anti-FcgRIIB).

Journal Pre-proof

These data suggest that a vast array of an intracellular signaling pathway is activated to modulate the action of distinct immune cells during asthma exacerbations.

Expression of SARP and U-BIOPRED genes

Two large cohorts studies, SARP and U-BIOPRED, have identified 104 genes that are closely associated with the pathogenesis of severe form of asthma. We have found 10 genes were differentially expressed by identified cell clusters (Fig. 4). Among these genes, CEACAM8 and DPYSL3 were predominantly expressed by macrophage clusters. AMPD3, ATXN7L1, and CHML were differentially expressed by macrophage, $CD4^+$ and $CD8^+$ T cell clusters. GSDMB was strongly expressed by T cell clusters, while HOMER2 by monocyte clusters. IL18R1 was mainly found in the $CD8^+$ T cell cluster. Interestingly, we were able to detect TSLP express in part of the macrophage cluster.

Gene network analyses

Gene set enrichment analysis was performed by using IPA with the "upstream regulator," "canonical pathway," and "diseases & function" options to understand the activation of intracellular molecular networks during an asthma exacerbation. C1-a ($CD8^+$ T cells), C6 (macrophage: monocyte−derived IL−4/Dex/TGFβ), C7 (monocyte:S_typhimurium_flagellin), CX-1 (a subpopulation of macrophage: alveolar) and CX-2 (a subpopulation of macrophage: alveolar) clusters were chosen as the proportion of these clusters was significantly elevated in the BALF of patients with asthma exacerbations when compared to those of healthy controls (Fig. 5). A total of 420 genes of C1-a ($CD8^+$ T cells), 97 gene of C6 (macrophage: monocyte−derived:IL−4/Dex/TGFβ), 428 genes of C7 (monocyte: S_typhimurium_flagellin), 107 genes of CX-1 (a subpopulation of macrophage: alveolar), and 167 gene of CX-2 (a subpopulation of macrophage: alveolar) that were differentially expressed by at least 2-fold in asthma exacerbations group were selected (Table E4).

Both C1-a (a subpopulation of $CD8^+$ T cells) and C7 (monocyte: S_typhimurium_flagellin) were more active as they had more upstream regulators when compared to C6 (macrophage: monocyte−derived:IL−4/Dex/TGFβ), CX-1 (a subpopulation of macrophage: alveolar), and CX-2 (a subpopulation of macrophage: alveolar) (Fig. 6A and Table E1). TNF, IFNγ, CAB39L and HIF1A were the top upstream regulators shared by C1-a (a subpopulation of $CD8^+$ T cells) and C7 (monocyte: S_typhimurium_flagellin) clusters, with high activation z-score. CCL5, RELA, ERBB2, PGR, IL-1A, IL-1B were uniquely and strongly detected in C7 (monocyte: S_typhimurium_flagellin). JNK, CD40, PRL, STAT3, Myc, and SATB1 were employed by C1-a (a subpopulation of $CD8^+$ T cells), whereas PRL, Myc, and SATB1 were similarly used by CX-2 (a subpopulation of macrophage: alveolar). By contrast, there were three and two upstream regulators detected in C6 (macrophage: monocyte−derived:IL−4/Dex/TGFβ) and CX-1 (a subpopulation of macrophage: alveolar), respectively.

The subset of genes with the highest activation z score of canonical pathways was primarily involved with "EIF2 Signaling", followed by "Ephrin Receptor Signaling," "Signaling by Rho Family GTPase," and "CXCR4 Signaling" in both C1-a ($CD8^+$ T cells) and C7 (monocyte: S_typhimurium_flagellin) (Fig. 6B and Table E2). Indeed, the activation profiles of canonical pathways between C1-a (a subpopulation of $CD8^+$ T cells) and C7 (monocyte: S_typhimurium_flagellin) were highly similar. Although the top canonical pathway in C6 (macrophage: monocyte−derived:IL−4/Dex/TGFβ), CX-1 (a subpopulation of macrophage: alveolar) and CX-2 (a subpopulation of macrophage: alveolar) was "EIF2 Signaling", their top canonical pathways were different from, and the ratio and percentage of activation were lower than those of C1-a ($CD8^+$ T cells) and C7 (monocyte: S_typhimurium_flagellin).

Journal Pre-proof

Journal Pre-proof

386 The top overrepresented disease & function categories were shown in the five clusters
387 (Fig. 6C and Table E3). “Infection by RNA virus” was classified as the highest
388 overrepresented disease category in both C1-a (a subpopulation of macrophage: alveolar) and
389 C7 (monocyte: S_typhimurium_flagellin). While these 2 clusters also showed significant
390 association with “Infection of cells” and “Viral infection,” C1-a ($CD8^+$ T cells) exhibited a
391 strong association with “Infection by HIV-1”, “HIV infection,” and “Replication of influenza
392 A virus” and CX-2 (a subpopulation of macrophage: alveolar) with “Replication of RNA
393 virus.” Other categories of disease & function were linked to cell mobility and survival.
394 When considering the number of involved molecules and adjust P-value, the activation status
395 of C6 (macrophage:monocyte−derived:IL−4/Dex/TGFb), CX-1 and CX-2 (subpopulations of
396 macrophage:alveolar) was significantly lower than that of C1-a (a subpopulation of
397 macrophage:alveolar) and C7 (monocyte:S_typhimurium_flagellin).

Journal Pre-proof

Journal Pre-proof

DISCUSSION

Our study demonstrates the application of scRNA Seq of BALF immune profiles to further the understanding of the immune landscape in patients with asthma exacerbations. Identification pathways and molecular events underpinning asthma exacerbations are critical fields of interest in asthma research, however previous studies of asthma transcriptomic for the understanding of the cellular and molecular makeup of immune response in the lung have been more limited as there no adequate tools to investigate differences between histologically indistinguishable cells. Our results provide data-driven determination of a complex network of molecular responses that contribute to the pathogenesis of asthma exacerbations at single-cell level and decode the network by using IPA upstream regulator, canonical pathways and disease & function analysis. They dissect the multiple distinct biological pathways and the interaction among these pathways leading to an exacerbation.

Reference-based annotation of scRNA Seq is to label new cells from a dataset based on similarity to the reference dataset with known labels and to yield objective, scalable, and reproducible annotation (30). With SingleR, an automatic annotation method, we identified 69 cell clusters in the BALF samples that were refined to 16 major cell clusters. Furthermore, the levels of $CD8^+$ T cells, several monocyte clusters, and a monocyte-derived macrophage subpopulation increased in the BALF of patients with asthma exacerbations. Our observations are in line with multiple known mechanisms of asthma exacerbation, confirming their importance in this human study. One longitude study with asthmatic patients have shown that the decline in lung function is linked to the level of $CD8^+$ T cells in airway biopsies (31). In another study, virus-specific $CD8^+$ T cells are critical immune cells that are a surrogate for anti-infection activity and are known as potent IL-5 producers in the presence of Th2 cells (32), implying their role in asthma exacerbations. Monocytes accumulate in the lung of asthma patients and critically contribute to respiratory infection by the release of pro-

Journal Pre-proof

inflammatory factors (33). Although numerous immune cells are present in the airways of asthma patients, monocytes and macrophages are the most abundant cells whose levels are consistent across different phenotypes of asthma (34). We found that the levels of these cells are upregulated in exacerbations. This observation may provide a mechanism pivotal to the link between repeated exacerbations and a decline in lung function.

Interestingly, approximately 50% of C15 (neutrophils) actively produce IL-1β, while other cell clusters, including macrophage and monocyte clusters, also express this cytokine. IL-18 was more profoundly expressed by macrophage, monocyte and neutrophil clusters. Our observation is also corroborated by the research that the levels of IL-1β and IL-18 are significantly higher in human lung (35, 36). Mouse studies have shown that macrophage, monocyte -derive IL-1β and IL-18 contribute the asthma exacerbation, AHR, and airway inflammation (37, 38). We have also found that IL-27 was significantly expressed by C3 (macrophage: monocyte-derived:M-CSF/IFNγ) and C9 (monocyte: anti-FcgRIIB), both of which are monocyte origin. IL-27 and IFNγ are prominent cytokines involved in the Th1 response and anti-viral immunity. We have previously shown that these two cytokines critical regulate infection-associated steroid-resistant AHR and airway inflammation in mouse models of asthma exacerbations (39, 40). $CD8^+$ T cells strongly expressed IFNγ, other cell clusters, including macrophage, monocyte, memory B cells, NK cell, and neutrophils, also express IFNγ to a lesser extent. This may explain why it is so challenging to treat exacerbation as a great variety of immune cells that produce IFNγ. We have found that C0 (macrophage:alveolar) and C15 (neutrophil) only weakly express CCL24 and no cluster expresses IL-5, which could explain why there are few eosinophils in the BALF.

The secretion of pro-inflammatory molecules by immune cells in exacerbation activates a variety of downstream signaling pathways that trigger the development of the disease. There is a substantial expression of intracellular signaling regulators in the BALF

immune cells of the patients with asthma exacerbations. Although the expression pattern was not selective, these regulators expressed at much higher levels in specific cell clusters. For instance, RUNX1 and RUNX3 were highly expressed in neutrophil clusters, while other clusters also show these two factors at relatively lower levels. RUNX1 critically regulate hematopoiesis, and RUNX2 modulates osteogenesis (41, 42). RUNX1 is also associated with airway hyperresponsiveness in a study of pediatric asthma and promotes Th17 responses (43, 44). Importantly, the interaction between RUNX1, RUNX3, and T-bet (TBX21) plays an essential role in the generation of IFNγ-producing Th17 cells (45). To the best of our knowledge, this study is the first to demonstrate that both regulators are highly expressed in neutrophils in asthma exacerbations. Interestingly, multiple cell clusters also highly expressed T-bet, particularly in C14 (monocyte: $CD16^-$). Limited evidence is available for the role of T-bet in the regulation of $CD16^-$ monocytes, let alone asthma exacerbation. It appears that IFNγ but not IFNα, LPS, IL-1, and TNF rapidly and markedly increases the level of T-bet in cultured primary human $CD45^+CD14^+$ monocyte and a monocyte cell line (THP-1) (46). Although their activation is primarily regulated by phosphorylation, we found that many cell clusters express STAT1 to STAT6 at a variable degree. JAK-STAT signaling pathways that transduce cytokine-regulated signals have a critical and profound role in the pathogenesis of asthma by several mechanisms, including the regulation of Th1/Th2 differentiation, IgE production, and cytokine generation (47).

We have demonstrated that other intracellular regulators are highly expressed across many immune cell clusters in asthma exacerbations. Although their role in the exacerbation is less known as the aforementioned regulators, they are believed to contribute to the pathogenesis of asthma exacerbation. One of these factors, BALF, whose level increases in asthmatic children, plays a role in lymphocyte- and mast cell-associated immune response in asthma (48). BCL6 is known to control the stability of Tregs and to suppress Th2 response by

Journal Pre-proof

attenuating STAT5 and GATA3 binding to enhancer regions of Th2 cytokine gene loci (49). Interestingly, we also observed the expression of GATA3 and FoxP3 across several cell clusters, not limited to T cells. NF-κB is a well-known pro-inflammatory transcriptional pathway that modulates the function of a wide range of immune cells. HIF-1α, a hypoxia-inducible factor, importantly shapes the role of macrophages and neutrophils and contributes to the development of the inflammatory diseases, including asthma (50). In this study, we showed the differential expression of key components of NF-κB signaling molecules and HIF-1α across many cell clusters simultaneously, potentially providing a clue how these pathways function in asthma exacerbation. Needless to say, these signaling molecules form a highly complicated framework uniquely seen within each immune cell, which can be important targets for the treatment of the disease. Developing new agonists or antagonists against one or several signaling pathways by targeting specific immune cells provides a new approach for the treatment of asthma exacerbations.

By comparing with SARP and U-BIOPRED datasets of severe asthma, we have identified 10 genes our results. CHML was one of the genes expressed in almost all clusters. CHML, named as Rab proteins geranylgeranyltransferase component A2, regulates protein geranylgeranylation and plays a role in protein transportation via secretory and endocytosis pathways (51). Selective inhibition of protein geranylgeranylation attenuates eosinophilic inflammation in the lung in a mouse model of asthma (52). DPYSL3 is required for mitosis and migration and negatively regulates p21-activated kinase (PAK) (53). HOMER2 is linked to hearing loss, rectal carcinoma, and osteoarthritis. While HOMER2 and DPYSL3 have no known functions associated with asthma, our data clearly indicate the role of these two factors in the pathogenesis. Importantly, TSLP was found to be expressed in a part of the macrophage cluster. This cytokine than can be produced by epithelial cells, macrophages, and mast cells is known to regulate the function of T cells, ILC2s, and myeloid cells and is

implicated in the pathogenesis of allergic disorders (54). Although it remains unclear of the role of TSLP-producing macrophages in the lung, these cells may modulate the subsequent host responses through this cytokine.

We also determined that the level of five clusters increases significantly in the BALF of patients with asthma exacerbations. Therefore, their transcripts were further analyzed in silico for the interaction of intracellular signaling by using IPA. The analysis of the top upstream regulators, canonical pathways, and disease & function have revealed that several conservative pathways are presumed to play a role in the pathogenesis. Our data suggest that the coordination of multiple intracellular molecular hubs regulates host responses at single-cell level. IPA profiling with upstream regulators shed light on C1-a (a subpopulation of $CD8^+$ T cells) and C7 (monocyte: S_typhimurium_flagellin) as they had the highest activation z-score but also potentially activated by a group of regulators, including TNF, IFNγ, CAB39L, HIF1a, CSF2, and TGFb1. These molecules critically contribute to the pathogenesis of inflammation. Likewise, IPA profiling with canonical pathways and disease & function identified C1-a (a subpopulation of $CD8^+$ T cells) and C7 (monocyte: S_typhimurium_flagellin) as the most activated cell clusters. Both clusters had the highest activation z score with a high ratio of involved molecules and low P-value and shared similar profiles of canonical pathways and diseases & functions. Among those canonical pathways, activation of EIF2 signaling is crucial for stress-induced regulation of translation in mammalian cells and often occurs upon infection (55). Ephrin receptor signaling is required for cell migration, tissue homeostasis and development processes (56), whose dysfunction leads to multiple disease states including cancer and infectious diseases (57, 58). Other pathways, including Signaling by Rho family GTPase, CXCR4 signaling, cardiac hypertrophy signaling, RhoA signaling, and phospholipase C pathways, are likely conservatively employed by these two cell clusters for cell mobility, inflammatory responses,

and cytokine production. By using diseases & functions, it appears that C1-a (a subpopulation of $CD8^+$ T cells) and C7 (monocyte: S_typhimurium_flagellin) are potential key players in immunity against viral infection with a strong association with virus infection linked functions. It is well-known that respiratory viral infection triggers asthma exacerbation by promoting airway inflammation, mucus hypersecretion, and airway blockage. Both $CD8^+$ T cells and monocytes are the critical immune cells against viral infection as the former cells module virus clearance by directly killing virus-infected cells, and the latter cells generate type I IFN and cytokine response upon RNA virus infection through the activation of TLR7 and TLR8 (59). Furthermore, $CD8^+$ T cells are capable of producing either IL-5 or IL-13 (60, 61), suggesting their potential role in asthma exacerbation.

Our result indicates a broad array framework that is composed of cytokines, intracellular signaling transducers, and other functional proteins that underpins the development of asthma exacerbations. Although the analysis of these molecular networks of large-scale transcriptomic at a single-cell level will enhance the understanding of the pathophysiology of asthma exacerbation, it still has some limitations and challenges. First, the analysis of high-throughput genetic data is the inherent complexity of many biological processes and interaction among individual cells. Second, the role of interactions of protein-protein, protein-DNA, and protein-RNA and epigenetic regulators in the interaction should be elucidated for establishing such a molecular framework. Moreover, evaluating the specific function of a given molecule or a set of genes/protein is another facet for determining the viability of a possible model framework of intracellular events, as the cost and controllability in a lab setting need to be considered.

Furthermore, airway epithelial cells (AEC), airway smooth muscle (ASM) cells and fibroblasts can regulate subsequent immune response by the production of pro-inflammatory factors upon exposure to the infection of respiratory viruses (62-64). For example, human

Journal Pre-proof

ASM cells are potent producer of IL-6 family cytokines after infected with RSV or parainfluenza virus (65). Asthmatic airway fibroblasts that are infected with rhinovirus *in vitro* demonstrate the ability to regulate inflammation by the induction of pro-inflammatory factors (63, 66). Rhinovirus infected AEC express IL-33 that is an important cytokine for the induction of type 2 immunity (9). Eosinophil persistent infiltration has been demonstrated in airways after rhinovirus-induced experimental asthma exacerbation (67). Therefore, the viral infection transformed inflammatory responses in asthmatic lungs may amplify and perpetuate epithelial damage, mucus production and pathological airway narrowing, leading to the worsening of symptoms and frequent exacerbation. Thus, further investigation is needed to elucidate how these networks of immune cells and residential cells contribute to the course of the pathogenesis of asthma exacerbations at single cell level. Nevertheless, the growth in knowledge and technologies of improved prediction algorithms, transcriptomic and proteomic techniques, high throughput validation systems would enable the identification of key hub regulators at the single-cell level.

Respiratory viral infection, acute allergen exposure or inadequate compliance to asthma management regime may cause the exacerbation (1). Indeed, clinical trials on new biologics (e.g. anti-IL-5 and IL-5R) define the clinical features of patients and cellular infiltrates but do not define the exacerbation triggers (68, 69). The potential of heterogeneity of triggers in these cohorts may indicate why exacerbation rates are decreased but not eliminated within an individual cohort. The similar challenge in defining the patients as sub-populations in relation to a specific trigger in our study might suggest that inclusion of many patients with different exacerbation triggers might have limited to identify specific molecular pathways in response to specific triggers. Another limitation of this study is that we only compared the immune landscape of BALF between non-atopic healthy subjects and atopic patients with asthma exacerbation. In future, building on this data we will also attempt to

Journal Pre-proof

define unique mechanisms underpinning the trigger-specific exacerbations by patient stratification. Nevertheless, our molecular data represents episodes across the population with the potential to identify unified or common elements linked to these episodes of asthma exacerbation.

Our single-cell transcriptional analysis of the immune landscape in BALF of patients with asthma exacerbation provides an insightful framework for understanding the shared and distinct expression patterns of inflammatory genes at the individual cell level. Our study provides a cellular and molecular resource for understanding the role of the complex interaction between different host immune cells in the outcome of asthma exacerbations. It also serves as a basis to probe these immune interactions and to answer the questions how these immune cells with the same lineage acquire new functions in the new inflammatory niche or inherit unique functions from a distant origin. We believe that this unprecedented detail information is critical for understanding the pathogenesis of asthma exacerbation and for the development of advanced therapies for better control of the disease.

Journal Pre-proof

Journal Pre-proof

Acknowledgments

Single-cell deep sequencing using the BD Rhapsody analysis pipeline. This work was performed by Sinotech Genomics (Shanghai, P. R. China). We are grateful to Dr. Adam Collison and Professors Paul S. Foster and Peter Wark (University of Newcastle, Australia) for critically reading the manuscript.

Funding Support

This work was supported by a University-Hospital Joint Fostering Fund of Zhengzhou University (#23230016), China National Natural Science Foundation Project Grant (#81874042 and #81970030).

Journal Pre-proof

Journal Pre-proof

596 **REFERENCES**

597 1. Wark PA, Gibson PG. Asthma exacerbations . 3: Pathogenesis. Thorax.
598 2006;61(10):909-15.
599 2. Hansbro PM, Kim RY, Starkey MR, Donovan C, Dua K, Mayall JR, et al.
600 Mechanisms and treatments for severe, steroid-resistant allergic airway disease and asthma.
601 Immunol Rev. 2017;278(1):41-62.
602 3. Wenzel SE, Szefler SJ, Leung DY, Sloan SI, Rex MD, Martin RJ. Bronchoscopic
603 evaluation of severe asthma. Persistent inflammation associated with high dose
604 glucocorticoids. Am J Respir Crit Care Med. 1997;156(3 Pt 1):737-43.
605 4. Lambrecht BN, Hammad H. The immunology of asthma. Nat Immunol.
606 2015;16(1):45-56.
607 5. Hew M, Chung KF. Corticosteroid insensitivity in severe asthma: significance,
608 mechanisms and aetiology. Intern Med J. 2010;40(5):323-34.
609 6. Busse WW, Morgan WJ, Gergen PJ, Mitchell HE, Gern JE, Liu AH, et al.
610 Randomized trial of omalizumab (anti-IgE) for asthma in inner-city children. N Engl J Med.
611 2011;364(11):1005-15.
612 7. Pavord ID, Korn S, Howarth P, Bleecker ER, Buhl R, Keene ON, et al. Mepolizumab
613 for severe eosinophilic asthma (DREAM): a multicentre, double-blind, placebo-controlled
614 trial. Lancet. 2012;380(9842):651-9.
615 8. Castro M, Corren J, Pavord ID, Maspero J, Wenzel S, Rabe KF, et al. Dupilumab
616 Efficacy and Safety in Moderate-to-Severe Uncontrolled Asthma. N Engl J Med.
617 2018;378(26):2486-96.
618 9. Jackson DJ, Makrinioti H, Rana BM, Shamji BW, Trujillo-Torralbo MB, Footitt J, et
619 al. IL-33-dependent type 2 inflammation during rhinovirus-induced asthma exacerbations in
620 vivo. Am J Respir Crit Care Med. 2014;190(12):1373-82.

Journal Pre-proof

10. Chambers ES, Nanzer AM, Pfeffer PE, Richards DF, Timms PM, Martineau AR, et al. Distinct endotypes of steroid-resistant asthma characterized by IL-17A(high) and IFN-gamma(high) immunophenotypes: Potential benefits of calcitriol. J Allergy Clin Immunol. 2015;136(3):628-37 e4.

11. Message SD, Johnston SL. The immunology of virus infection in asthma. Eur Respir J. 2001;18(6):1013-25.

12. Farne HA, Johnston SL. Immune mechanisms of respiratory viral infections in asthma. Curr Opin Immunol. 2017;48:31-7.

13. Loza MJ, Djukanovic R, Chung KF, Horowitz D, Ma K, Branigan P, et al. Validated and longitudinally stable asthma phenotypes based on cluster analysis of the ADEPT study. Respir Res. 2016;17(1):165.

14. Bigler J, Boedigheimer M, Schofield JPR, Skipp PJ, Corfield J, Rowe A, et al. A Severe Asthma Disease Signature from Gene Expression Profiling of Peripheral Blood from U-BIOPRED Cohorts. Am J Respir Crit Care Med. 2017;195(10):1311-20.

15. Modena BD, Bleecker ER, Busse WW, Erzurum SC, Gaston BM, Jarjour NN, et al. Gene Expression Correlated with Severe Asthma Characteristics Reveals Heterogeneous Mechanisms of Severe Disease. Am J Respir Crit Care Med. 2017;195(11):1449-63.

16. Woodruff PG, Modrek B, Choy DF, Jia G, Abbas AR, Ellwanger A, et al. T-helper type 2-driven inflammation defines major subphenotypes of asthma. Am J Respir Crit Care Med. 2009;180(5):388-95.

17. Kuo CS, Pavlidis S, Loza M, Baribaud F, Rowe A, Pandis I, et al. A Transcriptome-driven Analysis of Epithelial Brushings and Bronchial Biopsies to Define Asthma Phenotypes in U-BIOPRED. Am J Respir Crit Care Med. 2017;195(4):443-55.

Journal Pre-proof

Journal Pre-proof

644 18. Reinke SN, Gallart-Ayala H, Gomez C, Checa A, Fauland A, Naz S, et al.
645 Metabolomics analysis identifies different metabotypes of asthma severity. Eur Respir J.
646 2017;49(3).
647 19. Chaussabel D, Baldwin N. Democratizing systems immunology with modular
648 transcriptional repertoire analyses. Nat Rev Immunol. 2014;14(4):271-80.
649 20. Eberwine J, Sul JY, Bartfai T, Kim J. The promise of single-cell sequencing. Nat
650 Methods. 2014;11(1):25-7.
651 21. Vieira Braga FA, Kar G, Berg M, Carpaij OA, Polanski K, Simon LM, et al. A
652 cellular census of human lungs identifies novel cell states in health and in asthma. Nat Med.
653 2019;25(7):1153-63.
654 22. Tibbitt CA, Stark JM, Martens L, Ma J, Mold JE, Deswarte K, et al. Single-Cell RNA
655 Sequencing of the T Helper Cell Response to House Dust Mites Defines a Distinct Gene
656 Expression Signature in Airway Th2 Cells. Immunity. 2019;51(1):169-84 e5.
657 23. Peters MC, Kerr S, Dunican EM, Woodruff PG, Fajt ML, Levy BD, et al. Refractory
658 airway type 2 inflammation in a large subgroup of asthmatic patients treated with inhaled
659 corticosteroids. J Allergy Clin Immunol. 2019;143(1):104-13 e14.
660 24. Reddel HK, Taylor DR, Bateman ED, Boulet LP, Boushey HA, Busse WW, et al. An
661 official American Thoracic Society/European Respiratory Society statement: asthma control
662 and exacerbations: standardizing endpoints for clinical asthma trials and clinical practice. Am
663 J Respir Crit Care Med. 2009;180(1):59-99.
664 25. Moore WC, Evans MD, Bleecker ER, Busse WW, Calhoun WJ, Castro M, et al.
665 Safety of investigative bronchoscopy in the Severe Asthma Research Program. J Allergy Clin
666 Immunol. 2011;128(2):328-36 e3.
667 26. Birey F, Andersen J, Makinson CD, Islam S, Wei W, Huber N, et al. Assembly of
668 functionally integrated human forebrain spheroids. Nature. 2017;545(7652):54-9.

Journal Pre-proof

669 27. Tirosh I, Izar B, Prakadan SM, Wadsworth MH, Treacy D, Trombetta JJ, et al.
670 Dissecting the multicellular ecosystem of metastatic melanoma by single-cell RNA-seq.
671 Science. 2016;352(6282):189.
672 28. Kramer A, Green J, Pollard J, Jr., Tugendreich S. Causal analysis approaches in
673 Ingenuity Pathway Analysis. Bioinformatics. 2014;30(4):523-30.
674 29. DePasquale EAK, Schnell DJ, Van Camp P-J, Valiente-Alandí Í, Blaxall BC, Grimes
675 HL, et al. DoubletDecon: Deconvoluting Doublets from Single-Cell RNA-Sequencing Data.
676 Cell Reports. 2019;29(6):1718-27.e8.
677 30. Aran D, Looney AP, Liu L, Wu E, Fong V, Hsu A, et al. Reference-based analysis of
678 lung single-cell sequencing reveals a transitional profibrotic macrophage. Nature
679 immunology. 2019;20(2):163-72.
680 31. Noble A, Mehta H, Lovell A, Papaioannou E, Fairbanks L. IL-12 and IL-4 activate a
681 CD39-dependent intrinsic peripheral tolerance mechanism in CD8(+) T cells. Eur J Immunol.
682 2016;46(6):1438-48.
683 32. Coyle AJ, Erard F, Bertrand C, Walti S, Pircher H, Le Gros G. Virus-specific CD8+
684 cells can switch to interleukin 5 production and induce airway eosinophilia. J Exp Med.
685 1995;181(3):1229-33.
686 33. Bousquet J, Chanez P, Campbell AM, Lacoste JY, Poston R, Enander I, et al.
687 Inflammatory processes in asthma. Int Arch Allergy Appl Immunol. 1991;94(1-4):227-32.
688 34. Simpson JL, Scott R, Boyle MJ, Gibson PG. Inflammatory subtypes in asthma:
689 assessment and identification using induced sputum. Respirology. 2006;11(1):54-61.
690 35. Borish L, Mascali JJ, Dishuck J, Beam WR, Martin RJ, Rosenwasser LJ. Detection of
691 alveolar macrophage-derived IL-1 beta in asthma. Inhibition with corticosteroids. J Immunol.
692 1992;149(9):3078-82.

Journal Pre-proof

Journal Pre-proof

693 36. Tanaka H, Miyazaki N, Oashi K, Teramoto S, Shiratori M, Hashimoto M, et al. IL-18
694 might reflect disease activity in mild and moderate asthma exacerbation. J Allergy Clin
695 Immunol. 2001;107(2):331-6.
696 37. Johnson VJ, Yucesoy B, Luster MI. Prevention of IL-1 signaling attenuates airway
697 hyperresponsiveness and inflammation in a murine model of toluene diisocyanate-induced
698 asthma. J Allergy Clin Immunol. 2005;116(4):851-8.
699 38. Hayashi N, Yoshimoto T, Izuhara K, Matsui K, Tanaka T, Nakanishi K. T helper 1
700 cells stimulated with ovalbumin and IL-18 induce airway hyperresponsiveness and lung
701 fibrosis by IFN-gamma and IL-13 production. Proc Natl Acad Sci U S A.
702 2007;104(37):14765-70.
703 39. Li JJ, Wang W, Baines KJ, Bowden NA, Hansbro PM, Gibson PG, et al. IL-27/IFN-
704 gamma induce MyD88-dependent steroid-resistant airway hyperresponsiveness by inhibiting
705 glucocorticoid signaling in macrophages. J Immunol. 2010;185(7):4401-9.
706 40. Nguyen TH, Maltby S, Tay HL, Eyers F, Foster PS, Yang M. Identification of IFN-
707 gamma and IL-27 as Critical Regulators of Respiratory Syncytial Virus-Induced
708 Exacerbation of Allergic Airways Disease in a Mouse Model. J Immunol. 2018;200(1):237-
709 47.
710 41. Okuda T, van Deursen J, Hiebert SW, Grosveld G, Downing JR. AML1, the target of
711 multiple chromosomal translocations in human leukemia, is essential for normal fetal liver
712 hematopoiesis. Cell. 1996;84(2):321-30.
713 42. Ducy P, Zhang R, Geoffroy V, Ridall AL, Karsenty G. Osf2/Cbfa1: a transcriptional
714 activator of osteoblast differentiation. Cell. 1997;89(5):747-54.
715 43. Haley KJ, Lasky-Su J, Manoli SE, Smith LA, Shahsafaei A, Weiss ST, et al. RUNX
716 transcription factors: association with pediatric asthma and modulated by maternal smoking.
717 Am J Physiol Lung Cell Mol Physiol. 2011;301(5):L693-701.

Journal Pre-proof

718 44. Zhang F, Meng G, Strober W. Interactions among the transcription factors Runx1,
719 RORgammat and Foxp3 regulate the differentiation of interleukin 17-producing T cells. Nat
720 Immunol. 2008;9(11):1297-306.
721 45. Wang Y, Godec J, Ben-Aissa K, Cui K, Zhao K, Pucsek AB, et al. The transcription
722 factors T-bet and Runx are required for the ontogeny of pathogenic interferon-gamma-
723 producing T helper 17 cells. Immunity. 2014;40(3):355-66.
724 46. Lighvani AA, Frucht DM, Jankovic D, Yamane H, Aliberti J, Hissong BD, et al. T-
725 bet is rapidly induced by interferon-gamma in lymphoid and myeloid cells. Proc Natl Acad
726 Sci U S A. 2001;98(26):15137-42.
727 47. Pernis AB, Rothman PB. JAK-STAT signaling in asthma. J Clin Invest.
728 2002;109(10):1279-83.
729 48. Ubel C, Sopel N, Graser A, Hildner K, Reinhardt C, Zimmermann T, et al. The
730 activating protein 1 transcription factor basic leucine zipper transcription factor, ATF-like
731 (BATF), regulates lymphocyte- and mast cell-driven immune responses in the setting of
732 allergic asthma. J Allergy Clin Immunol. 2014;133(1):198-206 e1-9.
733 49. Ogasawara T, Hatano M, Satake H, Ikari J, Taniguchi T, Tsuruoka N, et al.
734 Development of chronic allergic responses by dampening Bcl6-mediated suppressor activity
735 in memory T helper 2 cells. Proc Natl Acad Sci U S A. 2017;114(5):E741-E50.
736 50. Lin N, Simon MC. Hypoxia-inducible factors: key regulators of myeloid cells during
737 inflammation. J Clin Invest. 2016;126(10):3661-71.
738 51. Watanabe M, Fiji HD, Guo L, Chan L, Kinderman SS, Slamon DJ, et al. Inhibitors of
739 protein geranylgeranyltransferase I and Rab geranylgeranyltransferase identified from a
740 library of allenoate-derived compounds. J Biol Chem. 2008;283(15):9571-9.

Journal Pre-proof

52. Chiba Y, Sato S, Misawa M. GGTI-2133, an inhibitor of geranylgeranyltransferase, inhibits infiltration of inflammatory cells into airways in mouse experimental asthma. Int J Immunopathol Pharmacol. 2009;22(4):929-35.

53. Matsunuma R, Chan DW, Kim BJ, Singh P, Han A, Saltzman AB, et al. DPYSL3 modulates mitosis, migration, and epithelial-to-mesenchymal transition in claudin-low breast cancer. Proc Natl Acad Sci U S A. 2018;115(51):E11978-E87.

54. Ziegler SF. Thymic stromal lymphopoietin and allergic disease. J Allergy Clin Immunol. 2012;130(4):845-52.

55. Shrestha N, Bahnan W, Wiley DJ, Barber G, Fields KA, Schesser K. Eukaryotic initiation factor 2 (eIF2) signaling regulates proinflammatory cytokine expression and bacterial invasion. The Journal of biological chemistry. 2012;287(34):28738-44.

56. Lisabeth EM, Falivelli G, Pasquale EB. Eph receptor signaling and ephrins. Cold Spring Harb Perspect Biol. 2013;5(9).

57. Chen J, Sathiyamoorthy K, Zhang X, Schaller S, Perez White BE, Jardetzky TS, et al. Ephrin receptor A2 is a functional entry receptor for Epstein-Barr virus. Nat Microbiol. 2018;3(2):172-80.

58. Pasquale EB. Eph receptors and ephrins in cancer: bidirectional signalling and beyond. Nat Rev Cancer. 2010;10(3):165-80.

59. de Marcken M, Dhaliwal K, Danielsen AC, Gautron AS, Dominguez-Villar M. TLR7 and TLR8 activate distinct pathways in monocytes during RNA virus infection. Sci Signal. 2019;12(605).

60. Fuschiotti P, Larregina AT, Ho J, Feghali-Bostwick C, Medsger TA, Jr. Interleukin-13-producing CD8+ T cells mediate dermal fibrosis in patients with systemic sclerosis. Arthritis Rheum. 2013;65(1):236-46.

Journal Pre-proof

765 61. Stoeckle C, Simon HU. CD8(+) T cells producing IL-3 and IL-5 in non-IgE-mediated
766 eosinophilic diseases. Allergy. 2013;68(12):1622-5.
767 62. Oliver BG, Johnston SL, Baraket M, Burgess JK, King NJ, Roth M, et al. Increased
768 proinflammatory responses from asthmatic human airway smooth muscle cells in response to
769 rhinovirus infection. Respir Res. 2006;7:71.
770 63. Bedke N, Haitchi HM, Xatzipsalti M, Holgate ST, Davies DE. Contribution of
771 bronchial fibroblasts to the antiviral response in asthma. J Immunol. 2009;182(6):3660-7.
772 64. Lopez-Souza N, Favoreto S, Wong H, Ward T, Yagi S, Schnurr D, et al. In vitro
773 susceptibility to rhinovirus infection is greater for bronchial than for nasal airway epithelial
774 cells in human subjects. J Allergy Clin Immunol. 2009;123(6):1384-90 e2.
775 65. Elias JA, Wu Y, Zheng T, Panettieri R. Cytokine- and virus-stimulated airway smooth
776 muscle cells produce IL-11 and other IL-6-type cytokines. Am J Physiol. 1997;273(3 Pt
777 1):L648-55.
778 66. Ghildyal R, Dagher H, Donninger H, de Silva D, Li X, Freezer NJ, et al. Rhinovirus
779 infects primary human airway fibroblasts and induces a neutrophil chemokine and a
780 permeability factor. J Med Virol. 2005;75(4):608-15.
781 67. Fraenkel DJ, Bardin PG, Sanderson G, Lampe F, Johnston SL, Holgate ST. Lower
782 airways inflammation during rhinovirus colds in normal and in asthmatic subjects. Am J
783 Respir Crit Care Med. 1995;151(3 Pt 1):879-86.
784 68. Bleecker ER, FitzGerald JM, Chanez P, Papi A, Weinstein SF, Barker P, et al.
785 Efficacy and safety of benralizumab for patients with severe asthma uncontrolled with high-
786 dosage inhaled corticosteroids and long-acting beta2-agonists (SIROCCO): a randomised,
787 multicentre, placebo-controlled phase 3 trial. Lancet. 2016;388(10056):2115-27.

Journal Pre-proof

69. Ortega HG, Liu MC, Pavord ID, Brusselle GG, FitzGerald JM, Chetta A, et al. Mepolizumab treatment in patients with severe eosinophilic asthma. N Engl J Med. 2014;371(13):1198-207.

Journal Pre-proof

Journal Pre-proof

Figure Legends

Table 1. Clinical characteristics of the participants in the study

Figure 1. Heatmap of SingleR annotation. Scores derived by reference to the ImmGen database with clusters superimposed on the t-SNE plot.

Figure 2. Single-cell RNA-seq analysis of lung immune cells in BALF of asthma exacerbation. Single-cell RNA-seq was performed on single-cell suspensions generated from five lungs of a healthy subject and 11 lungs of patients with asthma exacerbations. Cells were clustered using a graph-based shared nearest neighbor clustering approach and plotted by a t-distributed Stochastic Neighbor Embedding (tSNE) plot. (A) 16 cellular populations identified. (B) tSNE plots of lung immune cells of Health and asthma exacerbation groups. Cell types were classified as indicated in the legend. (C) The expression level of IL-1α, IL-1β, IL-6, IL-18, TSLP, IL-27, CCL2, CCL5, CCL24, IFNγ, TNF, TGFβ1, and TGFβ2 are shown. Each dot is sized to represent the proportion of cells of each type expressing the marker gene and colored to represent the mean expression of each marker gene across all cells, as shown in the key. Other known cytokines including IL-2, IL-3, IL-4, IL-5, IL-12b, IL-17A, IL-22, IL-23, IL-25, IL-33, IL-36, CCL11 are not detected.

Figure 3. Dot plots representing the expression level of known transcriptional regulators associated with asthma exacerbation. The expression levels of known transcriptional regulators are shown. Each dot is sized to represent the proportion of cells of each type expressing the marker gene and colored to represent the mean expression of each marker gene across all cells, as shown in the key.

Journal Pre-proof

Figure 4. Single-Cell RNA-seq identify expression of severe asthma-associated genes in BALF immune cells.

Gene expression features in tSNE map of differentially expressed genes in the BALF immune cells of patients with asthma exacerbations.

Figure 5. tSNE plots of C1-a, C6, C7, CX-1 and CX-2 cell clusters of lung immune cells in BALF of asthma exacerbation. Cells were clustered using a graph-based shared nearest neighbor clustering approach and plotted by a t-distributed Stochastic Neighbor Embedding (tSNE) plot. tSNE plots of C1-a, C6, C7, CX-1 and CX-2 cell clusters of lung immune cells of Health and asthma exacerbation groups are shown. C1-a (a subpopulation of $CD8^+$ T cells); C6 (macrophage:monocyte−derived:IL−4/Dex/TGFb); C7 (monocyte:S_typhimurium_flagellin); CX-1 and CX-2 (subpopulations of macrophage:alveolar).

Figure 6. Top upstream regulator, canonical pathway, and diseases & functions analysis C1-a, C6, C7, CX-1 and CX-2.

(A) Predicted upstream regulators, (B) canonical pathways and (C) diseases & functions in C1-a, C6, C7, CX-1 and CX-2 clusters of BALF immune cells of patients with asthma exacerbations, generated by IPA analysis. p-value is shown for each regulator and pathway, as indicated in the color key. The ratio represents the number of genes from the list that maps to the pathway divided by the total number of genes that map to the same pathway. Each dot is sized to represent the proportion of cells of each type expressing the marker gene and colored to represent the mean expression of each marker gene across all cells, as shown in the key. C1-a (a subpopulation of $CD8^+$ T cells); C6

(macrophage:monocyte−derived:IL−4/Dex/TGFb); C7 (monocyte:S_typhimurium_flagellin); CX-1 and CX-2 (subpopulations of macrophage:alveolar).

Journal Pre-proof

Journal Pre-proof

TABLE 1. Clinical characteristics of the participants in the study

	Healthy	Asthma exacerbation	P value
NO#	5	11	
Age (y), mean (SEM)	44.4(5.988)	42.91(4.08)	0.9348
Sex, M/F	3/2	6/5	
BMI (kg/m2), mean (SEM)	24.31(1.157)	24.02(0.6035)	0.7427
Blood cell counts (×106/L)			
Total white blood cells(×10^9/L), Mean (SEM)	5.280(0.5472)	7.313(0.5688)	0.0355
Neutrophils(×10^9/L), Mean (SEM)	2.864(0.2805)	4.375(0.445)	0.0517
Eosinphils(×10^9/L), Mean (SEM)	0.088(0.03089)	0.3909(0.1597)	0.2102
Monocytes, Mean (SEM)	0.44(0.08695)	0.4791(0.03304)	0.2786
Lymphocytes, Mean (SEM)	1.858(0.2103)	2.038(0.2052)	0.5096
Spirometry			
FEV1 (% predicted)	113.9(11.75)	85.76(4.85)	0.0517
FVC (% predicted)	109.5(10.29)	103.1(4.532)	0.5833
FEV1/FVC ratio	99.39(2.940)	70.99(2.132)	0.0005
FEV1 % <80, no. (%)	(0/5)	(5/11)	
Serum IgE (IU/ml)	46.2(17.98)	358.5(155.6)	0.0517
FENO (ppb), Median (Q1-Q3)	14.6(2.4)	56.82(14.6)	0.0359
No. of sIgEs (of 15)	0.2(0.2)	2.273(0.6618)	0.0495
ACT score	N/A	14.36(1.545)	
Severity ATS/ERS criteria			
Mild	N/A	4	
Moderate	N/A	3	
Severe	N/A	4	
Asthma exacerbations in past year, NO#.			
No exacerbation	N/A	0	
One to 2 exacerbations	N/A	5	
More than 2 exacerbations	N/A	6	
Necessitating hospitalization in past year, NO#	N/A	5/11	
Necessitating ED visit in past year, NO#	N/A	2/11	
Age of asthma onset (y), Mean (SEM)	N/A	36.9(5.048)	

Journal Pre-proof

Journal Pre-proof

Table E1: List of top upstream regulators in C1-a, C6, C7, CX-1 and CX-2 clusters of BALF immune cells of patients with asthma exacerbations.

C1-a (a subpopulation of $CD8^+$ T cells); C6 (macrophage:monocyte−derived:IL−4/Dex/TGFb); C7 (monocyte:S_typhimurium_flagellin); CX-1 and CX-2 (subpopulations of macrophage:alveolar).

Journal Pre-proof

Journal Pre-proof
© 2000-2019 QIAGEN. All rights reserved.

Pathway	P	Score
IFNG	0.000159	3.743
SMARCA4	6.94E-08	3.606
CAB39L	3.54E-08	3
HSP90B1	3.56E-09	3
SYVN1	0.00117	3
MYC	9.61E-09	2.899
CEBPA	0.000845	2.828
TNF	0.00574	2.818
CSF2	0.00154	2.813
HIF1A	0.000103	2.711
PRL	0.00133	2.607
EGFR	0.0054	2.575
SATB1	1.08E-05	2.494
P38 MAPK	0.0319	2.425
ERK	0.0166	2.415
Jnk	5.28E-05	2.396
CD40	0.00252	2.391
TGFB1	0.00926	2.311
STAT3	0.00458	2.281
CD24	0.0487	2.236

Journal Pre-proof

Journal Pre-proof
© 2000-2019 QIAGEN. All rights reserved.

Pathway	P	Score
TGM2	1.62E-03	2.236
EGFR	1.15E-03	1.949
MAPK1	7.00E-03	1.154
PI3K (famil	8.35E-04	0.851
TP53	8.26E-03	0.684
ESR1	3.71E-03	0.293

Journal Pre-proof

Journal Pre-proof
© 2000-2019 QIAGEN. All rights reserved.

Pathway	P	Score
TNF	1.21E-14	5.231
CCL5	2.39E-14	3.742
CAB39L	1.99E-13	3.606
SYVN1	0.00000241	3.606
IFNG	0.000006	3.595
SMARCA4	7.30E-09	3.499
RELA	4.73E-11	3.406
TGM2	0.0000125	3.347
HIF1A	3.92E-07	3.307
ERBB2	0.0131	3.273
PGR	3.58E-09	3.235
P38 MAPK	0.000013	3.221
TGFB1	6.12E-07	3.137
EGFR	4.47E-10	3.121
IL1A	0.0000103	3.088
IL1B	0.00000917	2.97
CSF2	0.000384	2.959
ECSIT	9.74E-10	2.927
GPER1	1.31E-07	2.909
TP73	0.000584	2.896

Journal Pre-proof

Journal Pre-proof
© 2000-2019 QIAGEN. All rights reserved.

Pathway	P	Score
TP53	0.013	0.199
SMARCA4	0.00443	1
MAPK1	0.0092	1.154

Journal Pre-proof

Journal Pre-proof
© 2000-2019 QIAGEN. All rights reserved.

Pathway	P	Score
TGM2	0.000754	2.646
SMARCA4	2.23E-07	2.333
SYVN1	0.0169	2
PRL	0.0036	1.959
EGFR	0.00863	1.949
MYC	0.000268	1.467
MAPK1	0.0442	1.154
PI3K (family)	0.000867	1.124
TP53	0.013	1.031
SATB1	0.00459	1.029
ESR1	0.0467	0.774
ERK1/2	0.00325	0.468
IL15	0.00919	0.132
TP63	0.0016	0.115

Journal Pre-proof

Journal Pre-proof

Table E2: List of top canonical pathways in C1-a, C6, C7, CX-1 and CX-2 clusters of BALF immune cells of patients with asthma exacerbations.

C1-a (a subpopulation of $CD8^+$ T cells); C6 (macrophage:monocyte−derived:IL−4/Dex/TGFb); C7 (monocyte:S_typhimurium_flagellin); CX-1 and CX-2 (subpopulations of macrophage:alveolar).

Journal Pre-proof

Journal Pre-proof
© 2000-2019 QIAGEN. All rights reserved.

Pathway	P	Ratio	Score
EIF2 Signaling	2.51E-82	3.76E-01	6.708
Integrin Signa	1.26E-11	1.12E-01	4.264
Leukocyte Ext	7.59E-09	9.84E-02	4.123
Ephrin Recep	4.07E-07	8.99E-02	4
Signaling by R	1.26E-12	1.08E-01	3.962
Cardiac Hype	2.40E-02	3.37E-02	3.873
Actin Cytoske	6.31E-13	1.17E-01	3.8
RhoA Signalin	2.00E-11	1.49E-01	3.771
IL-8 Signaling	2.88E-05	7.18E-02	3.606
Cardiac Hype	2.14E-04	5.96E-02	3.606
Regulation of	1.00E-12	1.93E-01	3.5
Rac Signaling	1.51E-06	1.09E-01	3.464
CXCR4 Signali	1.95E-05	7.93E-02	3.464
Phospholipas	1.58E-08	8.54E-02	3.357
ILK Signaling	1.29E-07	9.19E-02	3.357
CD28 Signalin	5.13E-08	1.22E-01	3.317
fMLP Signalin	8.13E-05	8.70E-02	3.162
Oxidative Phc	1.91E-04	8.65E-02	3
Role of NFAT	6.76E-04	6.25E-02	3
Cdc42 Signali	6.31E-12	1.47E-01	2.982

Journal Pre-proof

Journal Pre-proof
© 2000-2019 QIAGEN. All rights reserved.

Pathway	P	Ratio	Score
EIF2 Signaling	6.31E-19	0.0845	3.162
Signaling by R	6.61E-07	0.0375	2.828
RhoA Signalin	6.92E-07	0.0579	2.646
ILK Signaling	9.77E-07	0.0432	2.646
Regulation of	1.74E-06	0.0682	2.236
Cdc42 Signali	1.58E-05	0.0465	2.236
Tec Kinase Sig	0.00053703	0.0312	2.236
Production of	0.00102329	0.027	2.236
Integrin Signa	0.00162181	0.0244	2.236
Actin Cytoske	2.82E-06	0.0376	2.121
Fc_ Receptor-	0.00060256	0.043	2
Nitric Oxide S	0.00063096	0.0426	2
Rac Signaling	0.00112202	0.0364	2
Leukocyte Ext	0.00123027	0.0259	2
PI3K/AKT Sign	0.0020893	0.0308	2
Role of NFAT	0.00616595	0.0227	2
IL-8 Signaling	0.00870964	0.0205	2
Cardiac Hype	0.13396767	0.00842	2
NRF2-mediat	0.00012303	0.0323	1
Chemokine Si	0.00029512	0.0519	1

Journal Pre-proof

Journal Pre-proof
© 2000-2019 QIAGEN. All rights reserved.

Pathway	P	Ratio	Score
EIF2 Signaling	3.16E-88	0.394	5.98
Signaling by R	7.94E-11	0.1	4.583
RhoA Signalin	2.00E-09	0.132	4
IL-8 Signaling	6.31E-08	0.0923	4
Ephrin Recep	8.91E-08	0.0955	4
Fc_ Receptor-	3.72E-10	0.161	3.873
Rac Signaling	3.39E-08	0.127	3.742
Cdc42 Signali	3.80E-08	0.116	3.742
Regulation of	1.66E-10	0.17	3.606
CD28 Signalin	7.76E-09	0.13	3.606
ILK Signaling	8.13E-07	0.0865	3.606
Phospholipas	3.16E-05	0.065	3.606
Cardiac Hype	0.14487719	0.0274	3.606
CXCR4 Signali	4.68E-06	0.0854	3.464
Cardiac Hype	0.00081283	0.0553	3.317
Integrin Signa	2.51E-08	0.0927	3.3
Actin Cytoske	1.51E-09	0.0986	3.273
fMLP Signalin	7.76E-09	0.13	3.207
Actin Nucleat	1.07E-06	0.143	3.162
Oxidative Phc	3.89E-05	0.0962	3.162

Journal Pre-proof

Journal Pre-proof
© 2000-2019 QIAGEN. All rights reserved.

Pathway	P	Ratio	Score
EIF2 Signaling	3.16E-74	0.23	5.292
Signaling by R	1.23E-05	0.0333	2.646
RhoA Signalin	1.74E-05	0.0496	2.449
ILK Signaling	1.95E-05	0.0378	2.449
Regulation of	4.68E-05	0.0568	2
Cdc42 Signali	0.0002884	0.0388	2
Tec Kinase Sig	0.00588844	0.025	2
Integrin Signa	0.01348963	0.0195	2
Actin Cytoske	4.90E-05	0.0329	1.89

Journal Pre-proof

Journal Pre-proof
© 2000-2019 QIAGEN. All rights reserved.

Pathway	P	Ratio	Score
EIF2 Signaling	1.00E-62	0.235	5.292
Signaling by R	2.57E-10	0.0625	3.742
Integrin Signa	3.55E-08	0.0585	3.464
Actin Cytoske	5.01E-11	0.0704	3.357
Regulation of	2.00E-12	0.136	3.317
Ephrin Recep	7.76E-08	0.0618	3.317
Cdc42 Signali	2.69E-09	0.0853	3.162
Rac Signaling	7.76E-09	0.0909	3.162
RhoA Signalin	1.95E-08	0.0826	3.162
ILK Signaling	1.15E-07	0.0595	3
Leukocyte Ext	1.23E-05	0.0466	3
Actin Nucleat	4.27E-08	0.114	2.828
fMLP Signalin	2.00E-06	0.0696	2.828
CD28 Signalin	2.00E-06	0.0696	2.646
Tec Kinase Sig	2.69E-06	0.0562	2.646
Fc_ Receptor-	5.37E-06	0.0753	2.646
Phospholipas	1.35E-05	0.0407	2.646
IL-8 Signaling	9.33E-05	0.041	2.646
PAK Signaling	6.61E-06	0.0729	2.449
Agrin Interact	1.95E-05	0.0789	2.449

Journal Pre-proof

Journal Pre-proof

Table E3: List of top diseases & functions in C1-a, C6, C7, CX-1 and CX-2 clusters of BALF immune cells of patients with asthma exacerbations.

C1-a (a subpopulation of $CD8^+$ T cells); C6 (macrophage:monocyte−derived:IL−4/Dex/TGFb); C7 (monocyte:S_typhimurium_flagellin); CX-1 and CX-2 (subpopulations of macrophage:alveolar).

Journal Pre-proof

Journal Pre-proof
© 2000-2019 QIAGEN. All rights reserved.

Pathway	P	Score	MoleculeN
Migration of	1.86E-14	6.264	92
Cell movemer	1.91E-15	6.097	101
Viral Infectior	3.16E-19	6.014	104
Infection by R	1.22E-09	5.441	57
Cell viability	0.00000895	5.313	56
Cell movemer	3.22E-12	5.235	69
Migration of t	1.29E-09	5.117	57
Infection of c	1.18E-09	4.826	51
Infection by H	0.00000842	4.725	36
HIV infection	0.0000141	4.628	40
Leukocyte mi	4.30E-10	4.318	37
Cell movemer	9.10E-15	4.258	31
Cell movemer	3.40E-13	4.245	35
Chemotaxis	5.97E-07	4.219	26
Cell movemer	1.69E-10	4.152	38
Invasion of ce	3.61E-11	4.037	60
Invasion of tu	1.65E-09	4.007	53
Cell movemer	1.73E-15	3.898	27
Replication of	3.19E-08	3.828	24
Cell proliferat	2.54E-15	3.807	107

Journal Pre-proof

Journal Pre-proof
© 2000-2019 QIAGEN. All rights reserved.

Pathway	P	Score	MoleculeN
Invasion of tu	2.06E-08	3.512	20
Invasion of ce	5.70E-10	3.444	23
Cell movemer	0.000022	3.341	18
Cell proliferat	1.02E-08	3.082	31
Cell movemer	0.00000123	2.941	26
Migration of	0.00000762	2.9	23
Invasion of br	0.0000262	2.771	9
Invasion of pr	0.00000176	2.39	7
Proliferation	0.000048	1.746	8
Cell movemer	0.0000571	1.709	6
Organismal d	0.00000146	1.134	14
Epithelial-me	0.0000471	0.796	7
Synthesis of r	0.0000536	0.663	8
Synthesis of p	6.24E-16	0.156	20

Journal Pre-proof

Journal Pre-proof
© 2000-2019 QIAGEN. All rights reserved.

Pathway	P	Score	MoleculeN
Cell movemer	3.17E-21	6.698	114
Migration of	2.70E-19	6.574	103
Viral Infectior	2.43E-21	6.084	109
Cell movemer	4.94E-19	5.997	83
Migration of t	2.48E-17	5.934	73
Invasion of ce	6.41E-25	5.544	85
Invasion of tu	6.71E-20	5.085	73
Infection by R	1.35E-08	5.04	55
Infection of c	3.84E-08	5.024	48
Cell survival	7.36E-11	4.97	72
Cell viability c	3.99E-09	4.809	59
Cell viability	2.78E-10	4.724	69
Cell movemer	1.23E-16	4.272	48
Chemotaxis	1.31E-11	4.202	34
Leukocyte mi	3.52E-16	4.153	47
Replication of	1.83E-09	4.055	35
Cell movemer	7.85E-11	4.053	33
Migration of	1.08E-07	4.037	22
Activation of	6.83E-09	3.952	34
Cell movemer	8.34E-14	3.927	30

Journal Pre-proof

Journal Pre-proof
© 2000-2019 QIAGEN. All rights reserved.

Pathway	P	Score	MoleculeN
Invasion of tu	0.000439	3.516	14
Invasion of ce	0.00000734	3.398	18
Cell movemer	0.00511	3.203	14
Migration of t	0.00358	3.089	13
Cell movemer	0.00117	2.939	21
Viral Infectior	0.00000515	2.932	25
Cell proliferat	0.0000581	2.91	12
Replication of	0.000909	2.906	9
Migration of c	0.000736	2.734	20
Cell proliferat	0.0000979	2.488	25
Cell proliferat	0.000839	2.236	6
Chemotaxis	0.000829	2.191	8
Cell movemer	0.000301	2.017	7
Invasion of pr	0.0000381	2	6
Engulfment o	0.00202	1.982	4
Invasion of cc	0.00115	1.974	4
Chemotaxis o	0.00007	1.963	6
Inflammatory	0.000175	1.961	9
Replication of	0.000183	1.91	4
Organismal d	0.00147	1.633	10

Journal Pre-proof

Journal Pre-proof
© 2000-2019 QIAGEN. All rights reserved.

Pathway	P	Score	MoleculeN
Invasion of tu	3.52E-08	4.857	27
Invasion of ce	9.82E-10	4.779	31
Cell movemer	0.00000286	4.623	37
Cell movemer	0.0000172	4.523	26
Migration of	5.79E-07	4.449	36
Migration of t	0.00000355	4.361	25
Viral Infectior	1.28E-09	4.09	42
Cell proliferat	3.05E-08	3.555	21
Migration of	2.71E-07	3.539	13
Cell viability c	0.000272	3.475	22
Cell viability	0.000194	3.419	25
Cell proliferat	2.22E-08	3.375	44
Replication of	0.000836	3.367	12
Chemotaxis	0.00000451	3.241	14
Metabolism c	0.000596	3.124	11
Invasion of ca	0.0000848	3.105	10
Cell movemer	0.000445	3.083	11
Leukocyte mi	0.000112	3.034	14
Invasion of br	0.0000218	2.958	12
Cell movemer	0.00000803	2.957	9

Journal Pre-proof

Journal Pre-proof

Table E4: List of genes differentially expressed in C1-a, C6, C7, CX-1 and CX-2 clusters of BALF immune cells of patients with asthma exacerbations.

C1-a (a subpopulation of $CD8^+$ T cells); C6 (macrophage:monocyte−derived:IL−4/Dex/TGFb); C7 (monocyte:S_typhimurium_flagellin); CX-1 and CX-2 (subpopulations of macrophage:alveolar).

Journal Pre-proof

Journal Pre-proof

Gene_Symbol	Fold Changes (Log)
TRAF3IP3	0.69026569
GRAP2	0.69112585
ZFAS1	0.69209577
LSP1	0.69573617
NDUFA4	0.6969183
ZBTB7A	0.69695777
HMGB2	0.69759486
DDX46	0.69840845
RPL27AP	0.69965041
RPLP0	0.69990688
BAZ1B	0.69995033
PDIA3	0.70018254
ENO1	0.70063903
IVNS1ABP	0.70110308
SFPQ	0.70222531
MTDH	0.70501724
HCST	0.70530072
EVI2B	0.70553253
FYN	0.70575537
COX6B1	0.70590682
LASP1	0.70603011
PTGES3	0.70621056
CDC42SE1	0.7062294
CLK1	0.70674624
EWSR1	0.70808304
LENG8	0.7119289
COMMD6	0.71243025
SRSF3	0.71293976
LAPTM5	0.71497572
SMARCA2	0.71563016
LPXN	0.71708359
SSB	0.71880199
NDUFA1	0.72142409
CNN2	0.72149852
RPS26	0.72154799
SNHG5	0.72180334
FUS	0.72180489
DDX6	0.72451512
HLA.DRA	0.72502526
CDK6	0.72540355
LDHB	0.72546636
CIRBP	0.72554451
TMEM123	0.72967048
CD69	0.72991018
RP11.36C20.1	0.73003293

Journal Pre-proof

Journal Pre-proof

SLA	0.73211733
RPL35	0.73270458
ANXA2	0.73393236
RUNX3	0.73436162
SCAF11	0.73450077
PEBP1	0.73572338
TGOLN2	0.73650943
PPP2R5C	0.74286368
ANXA5	0.74294308
CALM2	0.74477895
OIP5.AS1	0.74738679
MAN1A2	0.75138512
C19orf43	0.75158893
UQCRB	0.75203084
IL7R	0.75361818
ZNF683	0.75572711
CAST	0.75877478
FNBP1	0.76254771
WAC	0.76331341
PPIG	0.76465389
ATP2B4	0.76570377
SH3KBP1	0.76837075
ITGA1	0.76871396
CAPZA1	0.76900062
PPP1R12A	0.77077353
HP1BP3	0.77309862
RP5.857K21.6	0.77633611
GMFG	0.7776447
SOD1	0.77793063
GPR171	0.778544
ADAR	0.78336103
ARID4B	0.78576432
PSAP	0.78577667
EZR	0.78632781
SPN	0.78733553
RAP1B	0.79070714
RP11.864N7.2	0.79108615
COX4I1	0.79174647
SERBP1	0.7929717
RSRP1	0.79376153
PDCD4	0.79394456
CMPK1	0.79880212
RBM25	0.79990378
AKAP9	0.80217577
PIP4K2A	0.80368872
MTRNR2L12	0.80668368

Journal Pre-proof

Journal Pre-proof

SRRM2	0.81059945
ZRANB2	0.81268532
DIAPH1	0.81284986
MBP	0.81305786
M6PR	0.81537564
TERF2IP	0.81608376
IFI16	0.81945684
S100A11	0.82115845
APOL6	0.82281954
HLA.J	0.82380108
MPHOSPH8	0.82537927
GAS5	0.82546224
EIF4B	0.82650686
CSDE1	0.82724616
SP100	0.82758278
CTSC	0.82837055
RPL6P27	0.83016273
SAMHD1	0.83217784
STK4	0.83649039
DEK	0.83657729
CYLD	0.84036601
OAZ1	0.84266093
FAM107B	0.84324157
ARGLU1	0.84344759
MYADM	0.84393076
BPTF	0.84622734
ARPC3	0.84982178
BCL11B	0.85119528
KPNB1	0.85200617
ATP6V0E1	0.85438774
ATRX	0.85488927
ATP5G2	0.85783541
TUBA1B	0.86172505
UBE2D3	0.86217936
GIMAP7	0.86487063
LCP2	0.86916596
COX6C	0.8700285
CAPZB	0.87022588
SUB1	0.87127267
HOPX	0.87227443
HNRNPD	0.87375636
APOBEC3C	0.87390567
CLIC1	0.87581261
RAB27A	0.87708706
KTN1	0.8774212
CXCR4	0.87834962

Journal Pre-proof

Journal Pre-proof

SNCRD3A	0.87914527
LTB	0.87918484
HLA.F	0.88012876
CBX3	0.88047467
NKTR	0.88172411
TAP1	0.88323305
HNRNPUL1	0.88340226
C9orf78	0.88503693
FAM129A	0.8903198
ATP5L	0.89077107
VAMP2	0.89377862
ROCK1	0.89471
GNG2	0.89722477
KHDRBS1	0.89723168
IKZF1	0.90202216
PNN	0.90359153
CCR5	0.90637099
IL2RB	0.90721432
RAD21	0.91192615
LUC7L3	0.91291133
TLN1	0.91304281
BCLAF1	0.91630047
GZMH	0.92211493
PGK1	0.92780358
ITGB2	0.92962852
SP110	0.93343967
SERF2	0.93965473
NUCKS1	0.94046662
ZFP36L2	0.94271132
MORF4L1	0.94517368
KLRD1	0.94643908
BRD2	0.94674134
RPL7	0.94706855
RP5.1052M9.	0.94764228
XAF1	0.95090874
PNISR	0.95426809
RP11.475C16	0.95467541
HLA.DPB1	0.95960231
UBC	0.96155631
IDS	0.96158881
HNRNPH1	0.96654409
N4BP2L2	0.96783274
CCND2	0.97246098
UBA52	0.97353037
LRRFIP1	0.97471652
NEAT1	0.97543383

Journal Pre-proof

Journal Pre-proof

RPL8	0.97652962
DAZAP2	0.98092941
HNRNPDL	0.98112431
PPP1R18	0.98364462
RPL36AL	0.98555744
IKZF3	0.9872947
RBM39	0.98954076
SLFN5	0.9932201
HCLS1	0.9943171
EIF4G2	1.00231638
ACTN4	1.00968495
CCL4	1.01169687
ARHGAP30	1.01236761
CLEC2D	1.01303361
HNRNPK	1.01660343
S100A10	1.01946933
JUN	1.02138806
COTL1	1.02372949
RPS9	1.02645599
YBX1	1.02853152
PCBP2	1.02871246
KMT2E	1.03240428
GNB1	1.03510801
HNRNPA3	1.03807027
TPM4	1.0415884
RPS28	1.04230827
HINT1	1.04374852
PRPF38B	1.04941273
APOBEC3G	1.05535376
RNF213	1.05696928
NKG7	1.0600659
CALR	1.06672468
MBNL1	1.06836445
RPL10	1.06868181
IFITM2	1.07595328
PIM1	1.0830557
PAG1	1.08795833
CD53	1.09222906
PSME1	1.10428248
SARAF	1.11451302
PCBP1	1.1158296
RASGRP1	1.11650591
CD63	1.11891779
ITM2B	1.11986793
HNRNPC	1.12388713
EIF3A	1.12897576

Journal Pre-proof

Journal Pre-proof

SYNE2	1.12998978
ANP32B	1.14283636
SRSF2	1.14349997
SRSF7	1.14627123
CELF2	1.14660741
EIF4A2	1.14830825
RP5.857K21.8	1.15698877
CAP1	1.1611851
ARF6	1.16856888
HLA.DRB1	1.17025824
CD96	1.17481383
MYH9	1.18053693
HNRNPU	1.19700798
ETS1	1.20116707
HMGB1	1.20235727
KMT2A	1.20487949
ARL4C	1.21051012
RPL22	1.21212996
HSP90B1	1.212145
SON	1.21434864
EEF1B2	1.2149391
EEF1D	1.21495025
NACA	1.22623416
RPL29	1.22702339
EMB	1.22947267
RPL36	1.23133449
SRSF5	1.234906
WIPF1	1.2363445
FTL	1.23682024
RP11.3P17.3	1.23689358
ACTR3	1.23816639
KIAA1551	1.24141607
SRGN	1.24256411
RPS5	1.24580175
Sep-07	1.24816466
TMSB10	1.25774721
RPL4	1.25875586
PRRC2C	1.25923318
TOMM7	1.2665833
MCL1	1.26686532
SRSF11	1.27313517
BTF3	1.27429977
HSPA8	1.27461424
TMBIM6	1.27978017
MYL12B	1.28725673
NPM1	1.29310711

Journal Pre-proof

Journal Pre-proof

TRGC2	1.29522015
RPL7A	1.30090146
RPL24	1.30372123
ACTR2	1.30729946
ALOX5AP	1.31854811
CD48	1.31945921
GAPDH	1.32081902
FAU	1.32315787
RHOA	1.32566184
ITGB1	1.32666459
CD3D	1.33539624
CDC42	1.33583155
CCNI	1.33686576
CD3G	1.34180608
PFDN5	1.34366066
RPSA	1.35402122
H3F3A	1.35504086
IQGAP1	1.36351553
ARL6IP5	1.36362502
RBPJ	1.37122046
SET	1.3784759
ZFP36L1	1.38193577
HNRNPA1	1.38196564
GZMA	1.38525492
TAGLN2	1.39716858
NCL	1.39996038
STK17B	1.406418
RPL23A	1.41396036
MYL12A	1.42005359
JUND	1.42188864
MSN	1.42635181
RPS2	1.43127914
HSP90AB1	1.43746934
RPS14	1.43795594
PPIA	1.43968906
CD44	1.45725645
ANKRD12	1.46315138
PLP2	1.47256312
RPL15	1.48530002
RPL26	1.50308038
BTG1	1.51357157
IL2RG	1.51413021
CD3E	1.51504585
S100A6	1.5285533
RACK1	1.54959292
RPS7	1.56631018

Journal Pre-proof

Journal Pre-proof

ANXA1	1.57997193
MYL6	1.58493095
RPL14	1.58632717
H3F3B	1.61513523
RPL13	1.62892275
DDX17	1.65280518
PTP4A2	1.67239737
SH3BGRL3	1.70624055
RPS4X	1.70749361
EIF1	1.72480444
CD99	1.74329155
DDX5	1.74583276
AHNAK	1.76321448
RPS13	1.76708946
NAP1L1	1.77147003
RPL12	1.7955909
HSP90AA1	1.80269919
RPL6	1.81113029
RPS18	1.81848481
HNRNPA2B1	1.82511939
RPS3A	1.83029355
RPL27	1.83064337
ARPC2	1.84608476
FTH1	1.86285058
RPL5	1.86650836
LCP1	1.86749576
RPL3	1.87083792
YWHAZ	1.88442882
CD8A	1.88822368
RPL19	1.89609103
ATP5E	1.89900982
RPLP1	1.9070868
TPM3	1.9112179
ARHGDIB	1.91700932
RPLP2	1.93872668
YWHAB	1.94953896
IL32	1.95136967
PABPC1	1.96868894
ID2	1.97708059
RPL10A	1.98601592
RPS15A	2.00535742
KLF6	2.03851721
RPS25	2.07084868
GNAS	2.08316177
RPS21	2.09662416
RPS3	2.13550962

Journal Pre-proof

Journal Pre-proof

RPS11	2.1442333
RPL39	2.16324221
FYB1	2.18727371
RPL11	2.19380905
RPS23	2.2021333
CD74	2.21280436
PTPRC	2.23860541
RPL35A	2.24187127
RPL38	2.24482183
VIM	2.27970634
CD2	2.32473634
TXNIP	2.34557828
RPS16	2.36518896
RPS19	2.36542013
PFN1	2.38139914
RPL41	2.43064354
RPL21	2.43746856
RPS20	2.47197906
CALM1	2.48207366
CD52	2.48909685
HLA.E	2.52181841
RPL13A	2.52617294
S100A4	2.55430641
RPL9	2.5629442
RP5.857K21.9	2.58179963
RPS12	2.67470105
CFL1	2.67658301
RPS24	2.68409136
RP5.857K21.1	2.73025562
TRAC	2.73359642
RPL37A	2.73404116
TRBC2	2.73608502
RPL23	2.77272152
ACTG1	2.83678447
RPL37	2.83955754
RPL32	2.84600464
RPL31	2.86907754
RPS8	2.89581416
CCL5	3.06232271
HLA.C	3.06899259
RPL27A	3.08685029
RPL30	3.13006469
RPL34	3.32119544
RPS27	3.3436068
RPS27A	3.40055858
PTMA	3.41691734

Journal Pre-proof

Journal Pre-proof

RPS6	3.44090753
RPS29	3.53949239
HLA.A	3.79351822
EEF1A1	3.89487036
TPT1	3.93020286
ACTB	3.96735343
HLA.B	4.13842377

Journal Pre-proof

Journal Pre-proof

Gene_Symbol	Fold Changes (Log)
CAPG	0.69742205
CALM1	0.70065733
FOS	0.70884782
HNRNPA2B1	0.71156985
ANKRD12	0.71994456
TMBIM6	0.72029223
PRRC2C	0.72392654
LGALS3	0.72598266
DDX17	0.73778416
FCGR3A	0.73910212
RPL11	0.74765731
CTSS	0.75010113
PPIG	0.75257137
CSTB	0.7694127
C1QC	0.77252211
RPS3	0.77421655
JUND	0.77917378
MTRNR2L12	0.78731741
CCDC88A	0.78974864
C1QA	0.79340316
RPL37	0.79453311
YWHAB	0.80632783
RPS6	0.80931079
RNF213	0.82328494
ANXA2	0.8249169
ATP5E	0.82630671
RPS27	0.82999027
HLA.E	0.83044635
ZC3H13	0.83135207
RPS16	0.83207124
RHOA	0.83675152
RPL31	0.85907527
RPL38	0.86355663
RPS8	0.86787041
ACTG1	0.86949615
ARPC2	0.86980708
VIM	0.88388011
HLA.DPA1	0.89219882
C1QB	0.8955283
HSP90AB1	0.89990997
RPL32	0.90996926
RPS24	0.9122699
MS4A7	0.93343838
FCER1G	0.9416632
LRRFIP1	0.94583477

Journal Pre-proof

Journal Pre-proof

LUC7L3	0.95084016
PNISR	0.95709215
HSP90B1	0.95925287
RPL30	0.96498991
RBM25	0.97427189
TAGLN2	0.97794102
CYBB	0.97837668
DDX5	0.99042317
MYL6	1.00365016
ABCG1	1.00805473
PABPC1	1.06172301
SRSF11	1.06561889
HLA.DRB5	1.08550319
RPL23	1.09292074
S100A4	1.0960631
S100A6	1.09708836
SERPINA1	1.10878966
CFL1	1.11821543
CTSB	1.12000947
RPS29	1.16609411
KLF6	1.17970028
PTMA	1.31234457
RPL27A	1.31364133
HLA.A	1.32339475
PSAP	1.35350803
TYROBP	1.38178976
HLA.DPB1	1.3873728
S100A11	1.41038258
RPL34	1.44149548
HLA.B	1.45061915
GRN	1.46527311
NEAT1	1.50135507
EEF1A1	1.55927414
PFN1	1.56184778
TXNIP	1.56220646
RP5.857K21.6	1.59509814
RP5.857K21.8	1.60041653
SAMHD1	1.67843651
LYZ	1.7253056
HSP90AA1	1.77927739
HLA.DRA	1.82694774
HLA.DRB1	2.10855342
TPT1	2.23678916
ACTB	2.29843803
FTH1	2.42454132
FTL	2.74295616

Journal Pre-proof

Journal Pre-proof

CD74	3.23352464
TMSB4X	3.31039067
B2M	3.40863015
RP5.857K21.1	3.45267029
RP5.857K21.9	4.08792347
MALAT1	5.20229011

Journal Pre-proof

Journal Pre-proof

Gene_Symbol	Fold Changes (Log)
ACTB	3.8402896
ACTG1	2.59581764
ACTR2	1.27650519
ACTR3	1.09357092
AHNAK	0.83628849
AIF1	1.15385764
AKAP13	0.72406562
ALCAM	0.7496303
ALDH2	0.76570126
ALOX5AP	0.9144558
ANKRD12	0.95822022
ANP32B	1.02571691
ANXA1	1.1493724
ANXA2	1.87591501
ANXA5	1.65680598
ARF6	0.8708679
ARHGDIB	1.11556583
ARL6IP5	0.82930314
ARPC2	1.92220649
ARPC3	1.42674204
ARPC5	0.97300394
ARRB2	0.76960488
ATF4	0.82039611
ATF5	0.70957531
ATP1B3	1.36155705
ATP2B1	0.72158062
ATP5E	1.87618176
ATP5G2	0.94938951
ATP5L	0.91630758
ATP6V0E1	0.85231135
ATP6V1B2	0.78398468
B2M	3.89675422
BASP1	0.75445344
BAZ1A	0.8445214
BHLHE40	0.90724902
BTF3	1.00477483
BTG1	1.24310775
C15orf48	1.18618792
C1orf162	0.75316386
CALM1	1.59790867
CALM2	1.1063608
CALR	1.29906805
CANX	0.99300388
CAP1	1.0120111
CAPG	0.78908918

Journal Pre-proof

Journal Pre-proof

CAPZA1	0.7908879
CAPZB	0.90669649
CAST	0.87953949
CCDC88A	1.2606428
CCL3	0.79396009
CCNI	1.28051205
CCNL1	0.84569772
CD4	0.76538673
CD44	1.49364933
CD52	0.82870194
CD53	0.89555502
CD63	1.55100692
CD74	4.56218466
CD83	1.09842024
CD86	1.01774419
CD9	0.8956211
CD99	0.81822074
CDC42	1.3143795
CDKN1A	1.16621103
CEBPB	0.76839479
CELF2	0.74100799
CFL1	2.54944686
CFLAR	0.76122854
CLIC1	0.80495405
CMIP	0.71343996
CMTM6	1.08959556
COTL1	1.3028816
COX4I1	1.03471779
COX6C	0.84549773
COX7C	0.80677668
COX8A	0.71559155
CSDE1	0.71616605
CST3	1.90684267
CSTB	1.34280272
CTSB	2.80647816
CTSC	0.8499545
CTSH	0.86366535
CTSL	1.01155286
CTSS	1.39468564
CTSZ	0.94905337
CXCL16	0.88683488
CXCR4	0.98955911
CYBB	1.16744409
DAZAP2	0.78484837
DBI	0.69831002
DDX17	0.94295755

Journal Pre-proof

Journal Pre-proof

DDX21	0.91254247
DDX5	1.57459526
DPYSL2	0.83358173
DUSP1	1.37313414
EEF1A1	3.51986311
EEF1B2	1.17160048
EEF1D	0.90536687
EEF2	0.78877035
EFHD2	0.89359939
EIF1	2.10709276
EIF2S2	0.71476431
EIF3A	0.92863499
EIF4A2	0.85199037
EIF4G2	1.06993212
EMP1	0.69460087
ENO1	0.83071852
ETV6	0.70586928
EZR	0.80062851
FABP5	0.69929761
FAU	1.24485345
FCER1G	1.97498858
FCGR2A	0.80280062
FGL2	0.76794298
FGR	1.02588534
FKBP1A	0.7698403
FOS	2.06516204
FOSB	0.88646749
FPR3	1.24648968
FTH1	3.77676897
FTHL10	1.32989927
FTHL20	0.89614572
FTL	2.55296238
FYB1	0.90115242
GAPDH	1.32001278
GDI2	1.00396456
GLIPR1	0.72774131
GLUL	1.00883985
GNAS	1.72769708
GNB1	0.87202073
GNG5	0.69874551
GPCPD1	0.73052923
GPR183	1.28745401
GRN	1.54561768
GSN	0.8648954
GSTO1	0.75847337
H2AFY	1.28902722

Journal Pre-proof

Journal Pre-proof

H3F3A	2.09800424
H3F3B	1.96681407
HBEGF	0.7078038
HCLS1	1.12260569
HINT1	0.718751
HLA.A	2.78156279
HLA.B	2.94076483
HLA.C	2.1118627
HLA.DMA	1.23774549
HLA.DMB	1.04019468
HLA.DPA1	2.90938034
HLA.DPB1	3.0266199
HLA.DQA1	2.30553837
HLA.DQB1	2.21182276
HLA.DRA	3.91162048
HLA.DRB1	3.7745712
HLA.DRB5	1.97668551
HLA.E	1.30551121
HMGB1	0.82134384
HNRNPA1	1.10997733
HNRNPA2B1	1.93746238
HNRNPA3	1.04929263
HNRNPC	1.06667075
HNRNPD	0.99362544
HNRNPDL	1.08906319
HNRNPH1	0.7992269
HNRNPK	1.02399478
HNRNPM	0.74465619
HNRNPU	0.97378766
HSP90AA1	2.41037159
HSP90AB1	1.81334704
HSP90B1	1.14150685
HSPA1A	0.90217143
HSPA5	1.01336362
HSPA8	1.12323887
ID2	0.9005875
IER2	0.73303432
IER3	1.21903713
IFI16	0.77036881
IFI6	1.18851339
IFITM3	0.98164608
IGSF6	1.05526997
IL1B	0.70218241
IL1RN	0.70898487
IL7R	0.96025751
IQGAP1	0.99121455

Journal Pre-proof

Journal Pre-proof

ITGB2	0.79118587
ITM2B	1.04760621
IVNS1ABP	0.78863782
JUN	1.11363539
JUNB	0.89012459
JUND	1.42090213
KIF5B	0.72460005
KLF4	0.70348418
KLF6	2.48060197
KTN1	0.89849368
LAPTM4A	0.7349771
LAPTM5	1.15908556
LCP1	1.68825037
LDHA	0.97549816
LGALS1	1.07046689
LGALS3	1.28644269
LIMS1	1.13036806
LITAF	1.66112045
LPXN	0.75290613
LRRFIP1	1.38000188
LST1	0.7589875
LYZ	3.01851846
M6PR	0.89361938
MALAT1	5.01794209
MARCKS	0.81273806
MCL1	1.46718974
MFSD1	0.77262049
MOB1A	0.8016042
MORF4L1	0.96407466
MS4A6A	0.97732387
MS4A7	1.03552333
MSN	0.86094919
MTDH	0.70566592
MTPN	0.77537788
MTRNR2L12	0.81135641
MYADM	0.83422921
MYL12A	0.75315968
MYL12B	0.97625667
MYL6	1.98767175
NACA	1.17425453
NAMPT	1.11777985
NAP1L1	1.62105899
NCL	0.96575358
NDUFA1	0.97598976
NDUFB2	0.76788303
NEAT1	2.30265552

Journal Pre-proof

Journal Pre-proof

NFKBIA	1.10309889
NPC2	1.20878583
NPM1	1.11596523
NR4A1	0.77235212
NR4A3	0.72907676
OAZ1	1.42282668
OLR1	1.32431797
PABPC1	2.62720587
PABPC4	0.8080059
PCBP1	1.13570796
PCBP2	1.03304964
PDIA3	0.8693238
PEA15	1.23363172
PFDN5	1.33372136
PFN1	2.50775862
PIM3	0.89529149
PKM	1.22134812
PLAUR	1.31869429
PLEK	1.36101895
PLP2	0.87252793
PLSCR1	1.06083732
PLXDC2	0.71255679
PNISR	1.04492169
PNRC1	0.84415243
PPIA	1.86823305
PPIG	0.72496201
PPP1R15A	0.69887078
PPT1	0.7043352
PRDX1	0.74820637
PRPF38B	0.7870019
PRRC2C	0.91190625
PSAP	2.50060861
PTBP3	0.73830578
PTMA	3.04342035
PTMAP5	0.79338204
PTP4A2	0.96250944
PTPRC	0.79967604
QKI	0.69380254
RAB31	0.89686287
RAB7A	0.77800054
RAC1	1.36075589
RACK1	1.41408089
RAN	0.85675651
RAP1B	0.79263981
RBM25	0.90865906
RBM3	1.21439416

Journal Pre-proof

Journal Pre-proof

RBM39	1.0585864
RBPJ	0.72332286
RGCC	0.91900669
RGS1	1.13765206
RGS10	0.75400501
RGS2	0.7358838
RHOA	1.35841521
RP11.3P17.3	0.80147903
RP11.475C16	0.77456982
RP11.864N7.2	0.80559803
RP5.1052M9.	0.91442783
RP5.857K21.1	2.76094682
RP5.857K21.6	1.09265496
RP5.857K21.8	1.0142042
RP5.857K21.9	3.27503667
RPL10	0.95295756
RPL10A	1.32815482
RPL11	1.78202775
RPL12	1.76987117
RPL13	1.27344614
RPL13A	1.56274512
RPL14	1.08074559
RPL15	1.30813309
RPL19	1.32571806
RPL21	2.02746079
RPL22	1.04206825
RPL23	2.58470001
RPL23A	0.92941565
RPL24	1.01927978
RPL26	1.4469681
RPL27	1.59249518
RPL27A	2.27245779
RPL29	1.03708917
RPL3	1.60483025
RPL30	2.14289228
RPL31	2.32823732
RPL32	2.20017283
RPL34	2.79434022
RPL35A	1.6275514
RPL36	1.1354851
RPL37	2.35057212
RPL37A	2.13495419
RPL38	1.85189987
RPL39	1.71436772
RPL4	1.26283142
RPL41	1.78838351

Journal Pre-proof

Journal Pre-proof

RPL5	1.55590057
RPL6	1.34081726
RPL6P27	0.91023111
RPL7	0.97541787
RPL7A	1.15918928
RPL8	1.16194911
RPL9	2.2392685
RPLP0	0.78731322
RPLP1	1.61598682
RPLP2	1.61781899
RPS11	1.72504219
RPS12	1.81528456
RPS13	2.01496076
RPS14	0.83438811
RPS15A	1.22979992
RPS16	2.35129131
RPS18	1.12421455
RPS19	1.80787441
RPS2	1.32214443
RPS20	2.07186479
RPS21	1.60306847
RPS23	1.87157637
RPS24	2.2855694
RPS25	1.31953619
RPS26	1.18316316
RPS27	1.77251195
RPS27A	2.16456786
RPS28	0.97462761
RPS29	2.62616215
RPS3	1.44414067
RPS3A	1.34247802
RPS4X	1.64147339
RPS5	1.12874724
RPS6	2.69692408
RPS7	1.19559051
RPS8	2.43581581
RPS9	1.22096482
RPSA	1.08079665
RTN4	1.43758201
S100A10	1.55009715
S100A11	2.22693088
S100A4	1.75761611
S100A6	1.7253893
S100A8	0.71358602
SAMHD1	1.93536578
SARAF	0.8242866

Journal Pre-proof

Journal Pre-proof

SAT1	2.01282889
SDCBP	1.03462478
SEM1	0.7049367
SERF2	1.36681817
SERPINA1	0.75071476
SERPINB1	1.0097224
SERPINB9	0.91625899
SET	0.8818729
SFPQ	0.96624347
SGK1	1.15889385
SH3BGRL3	1.04772764
SLC25A5	0.82587519
SLC25A6	0.81367746
SLC2A3	0.73113096
SNHG5	1.15635284
SNORD3A	0.76152103
SON	1.03695826
SPI1	0.96026691
SRGN	2.60778858
SRRM2	0.75002046
SRSF11	0.92207773
SRSF2	0.79730149
SRSF5	1.01670086
SUB1	0.80949268
SYNCRIP	0.73562367
TAGLN2	1.41688655
TGFBI	1.11954919
TMBIM6	1.3678127
TMSB10	1.49277356
TMSB4X	4.15250115
TOMM7	0.90435113
TPI1	0.72653093
TPM3	1.58212434
TPM4	1.17261359
TPT1	3.54611026
TUBA1A	0.74410628
TUBA1B	1.51933591
TXN	0.97876493
TXNIP	1.08146808
TYROBP	2.106046
UBA52	1.28355818
UBC	0.95470251
UBE2D3	0.95048057
UBXN4	0.69103267
UQCRB	0.7828748
VAMP8	0.87286595

Journal Pre-proof

Journal Pre-proof

VASP	0.78400665
VEGFA	1.13479898
VIM	2.84987465
VMP1	1.61076099
WSB1	0.91365114
YBX1	1.40052354
YWHAB	1.36117028
YWHAE	0.96157582
YWHAH	0.85687397
YWHAZ	1.52254759
ZEB2	0.83073119
ZFAND5	0.75665957
ZFAS1	0.79090594
ZFP36	1.98844127
ZFP36L1	1.25517266

Journal Pre-proof

Journal Pre-proof

Gene_Symbol	Fold Changes (Log)
ACTB	1.99371399
ACTG1	1.14236081
ANXA1	0.71350678
ANXA2	0.90495845
APOC1	0.89835056
ARPC2	0.71723015
ATP5E	1.19764769
B2M	3.33535944
C1QA	0.70222701
CALM1	0.72881367
CCNI	0.6950585
CD52	1.05855864
CD74	2.44492526
CFL1	1.50978452
COX6C	0.77161437
CSTB	0.91203274
CTB.36O1.5	0.77445372
CTSB	1.12345774
EEF1A1	2.3056223
FOS	0.81520928
FTH1	2.95615235
FTL	3.18416041
GNAS	0.85772581
H3F3A	0.76749722
HLA.A	1.40263106
HLA.B	1.65531985
HLA.C	1.02297147
HLA.DPB1	0.96525286
HLA.DRA	1.50884281
HLA.DRB1	1.15701278
HLA.DRB5	1.02348007
HSP90AA1	0.76098744
LGALS3	1.04053102
LYZ	1.70108382
MALAT1	2.06416193
MTRNR2L12	1.25712431
MYL6	0.70961469
NPM1	0.80876139
PABPC1	1.25506776
PFN1	1.41590633
PPIA	0.9326762
PSAP	0.99146597
PTMA	1.00218823
RP5.857K21.1	3.97244851
RP5.857K21.1	1.06852583

Journal Pre-proof

Journal Pre-proof

RP5.857K21.[illegible]	[illegible]
RP5.857K21.7	1.02687721
RP5.857K21.8	2.28330199
RP5.857K21.9	4.38755377
RPL10A	1.35130532
RPL11	1.39146684
RPL12	1.18220621
RPL13	0.81024069
RPL14	0.79070575
RPL19	0.74209622
RPL21	1.44807752
RPL23	1.80200396
RPL26	0.93706052
RPL27	0.71462562
RPL27A	1.59249526
RPL29	0.69286073
RPL30	1.77940415
RPL31	1.7327085
RPL32	1.66480059
RPL34	1.58989588
RPL35A	0.88964621
RPL37	1.72175358
RPL37A	1.54061519
RPL38	1.51311642
RPL39	1.13823724
RPL41	1.04487892
RPL5	0.88368568
RPL6	0.74862578
RPL9	1.41491614
RPLP1	0.85821871
RPLP2	1.02424503
RPS11	1.36991334
RPS12	1.56976581
RPS13	1.2682923
RPS15A	0.85569913
RPS16	1.35755383
RPS18	1.05983512
RPS19	1.10938078
RPS20	1.58814961
RPS21	1.37115298
RPS23	1.20526779
RPS24	1.20076224
RPS25	1.09973624
RPS26	0.79057045
RPS27	1.72367475
RPS27A	1.40220961

Journal Pre-proof

Journal Pre-proof

RPS29	2.16080959
RPS3	1.08657309
RPS4X	0.706484
RPS6	1.67635866
RPS8	1.93280867
S100A11	0.96910452
S100A4	1.28735345
S100A6	1.2217212
SAMHD1	0.92684942
TMSB10	0.72601843
TMSB4X	3.79703456
TOMM7	0.7099931
TPT1	2.66453762
TXNIP	1.14894274
VIM	0.92371476
YBX1	0.91289249

Journal Pre-proof

Journal Pre-proof

Gene_Symbol	Fold Changes (Log)
ACP5	1.26026782
ACTB	3.22631842
ACTG1	1.37175014
ACTR2	1.01945577
ALDH2	1.05615325
ANXA1	1.11360219
ANXA2	1.85193605
ANXA5	1.01510473
APOC1	1.53857591
ARPC2	1.09880899
ARPC3	0.77257521
ASAH1	0.79103832
ATP5E	1.66717386
ATP6V1F	0.76174508
B2M	3.58010124
BRI3	0.80011666
BTF3	0.78958213
C11orf58	0.74716717
CALM1	0.80893586
CALR	0.76303148
CAPG	0.71268691
CCNI	0.8900483
CD44	0.80265662
CD52	0.74830242
CD63	1.46260184
CD74	2.76032768
CDC42	0.83343364
CFL1	1.71964036
CIR1	0.80931732
CLTA	0.76394329
CSTB	2.72006768
CTSB	2.17040266
CTSD	1.0744702
CTSS	0.89141321
EEF1A1	2.59973742
EIF1	0.79429193
FBP1	0.7782269
FCER1G	1.05515405
FDX1	0.7430657
FOS	0.81745954
FTH1	4.2773485
FTHL10	0.9822994
FTHL20	0.7299018
FTL	4.11695031
GAPDH	0.92059134

Journal Pre-proof

Journal Pre-proof

GLUL	0.97139546
GM2A	0.77887713
GNAS	0.93486829
GPNMB	1.20245155
GPX1	0.88167052
GRN	1.64544125
GSTO1	1.3478812
H3F3B	0.77612191
HLA.A	1.96823727
HLA.B	1.58218702
HLA.C	1.21876143
HLA.DPA1	0.82006566
HLA.DPB1	0.79316773
HLA.DRA	1.8471216
HLA.DRB1	1.33017772
HLA.DRB5	1.15912694
HLA.E	1.06077382
HNRNPA2B1	1.18967922
HSP90AA1	1.85786927
HSP90AB1	0.9713624
ITGB1	0.77061065
KLF6	0.89632323
LGALS3	2.22833946
LITAF	0.87721792
LTA4H	0.91514209
LYZ	1.47294124
MALAT1	2.60187436
MS4A7	0.87007758
MTRNR2L12	1.0923019
MYL12B	0.84437526
MYL6	1.29860862
NEAT1	0.74361389
NOP10	0.69092353
NPC2	0.87714512
OAZ1	0.69063573
PABPC1	1.00067517
PFN1	2.26470177
PLIN2	0.99885481
PPIA	0.79040368
PRDX1	0.78515767
PSAP	1.93593694
PTMA	1.65628812
RAB7A	0.78345247
RAC1	0.80333531
RAP1B	0.74812318
RGCC	0.84757917

Journal Pre-proof

Journal Pre-proof

RHOA	1.07700004
RNF130	0.99482715
RP4.681N20.1	0.83800854
RP5.857K21.1	2.717576
RP5.857K21.6	1.02650148
RP5.857K21.8	1.24017008
RP5.857K21.9	3.95924587
RPL11	0.82222343
RPL12	0.80127558
RPL13	0.8298141
RPL13A	0.79190862
RPL19	1.33578356
RPL21	1.25967278
RPL23	2.10543185
RPL23A	0.77610454
RPL27	0.97560583
RPL27A	1.41314903
RPL29	0.92942253
RPL30	1.17337721
RPL31	1.60909679
RPL32	1.14672558
RPL34	2.15804688
RPL35A	0.77753235
RPL37	1.25438556
RPL37A	1.48770441
RPL38	1.06540784
RPL39	0.93168701
RPL41	1.00484485
RPL5	0.71840936
RPL6	0.8757267
RPL6P27	0.71749706
RPL9	1.58995103
RPLP1	0.8040575
RPLP2	0.76600676
RPS11	0.85614069
RPS12	1.42940687
RPS16	1.45626849
RPS18	1.03149722
RPS19	0.90901181
RPS2	0.83591633
RPS20	1.34498468
RPS21	0.8996915
RPS23	1.91065958
RPS24	1.16410462
RPS25	1.06922275
RPS26	1.16882178

Journal Pre-proof

Journal Pre-proof

RPS27	0.93424726
RPS27A	1.54321452
RPS29	1.43235558
RPS3	0.76441168
RPS4X	0.79773161
RPS6	2.12349905
RPS7	0.97748478
RPS8	1.35567501
S100A10	0.84148163
S100A11	1.88601521
S100A4	1.06087319
S100A6	2.18019401
SAMHD1	1.17519874
SAT1	0.69697945
SDCBP	0.8631546
SH3BGRL	0.7335527
TMBIM6	0.76816322
TMSB10	0.7715611
TMSB4X	3.43685886
TPM4	0.70089884
TPT1	2.7762198
TUBA1B	1.25050502
TXN	0.73872327
TXNIP	0.96098265
TYROBP	1.2931757
UQCRQ	0.78481918
VIM	2.17261785
YBX1	1.56034776
YWHAB	0.96210813
ZFP36L1	0.70308744

Journal Pre-proof

Journal Pre-proof

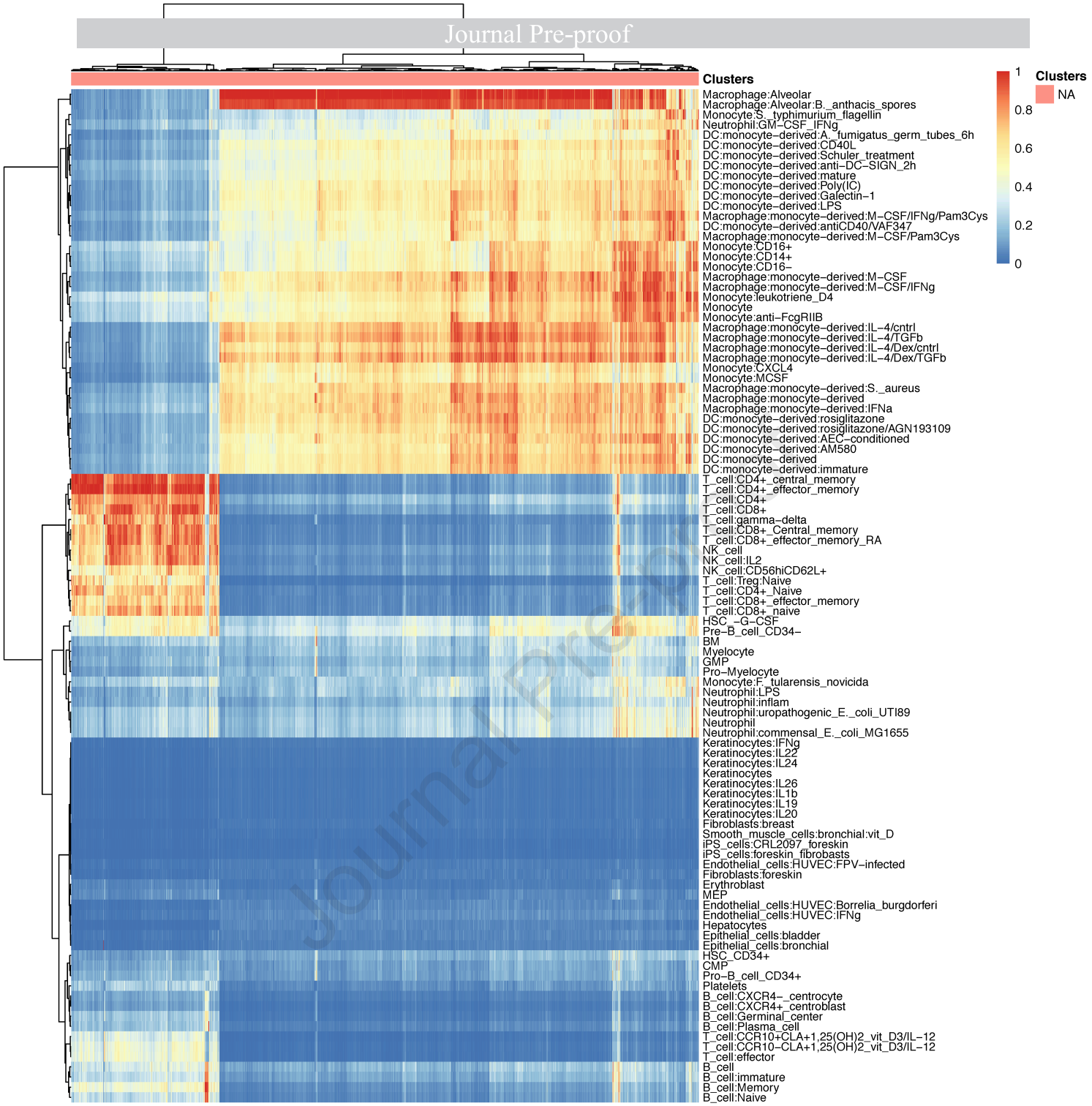


Fig 1.

Journal Pre-proof

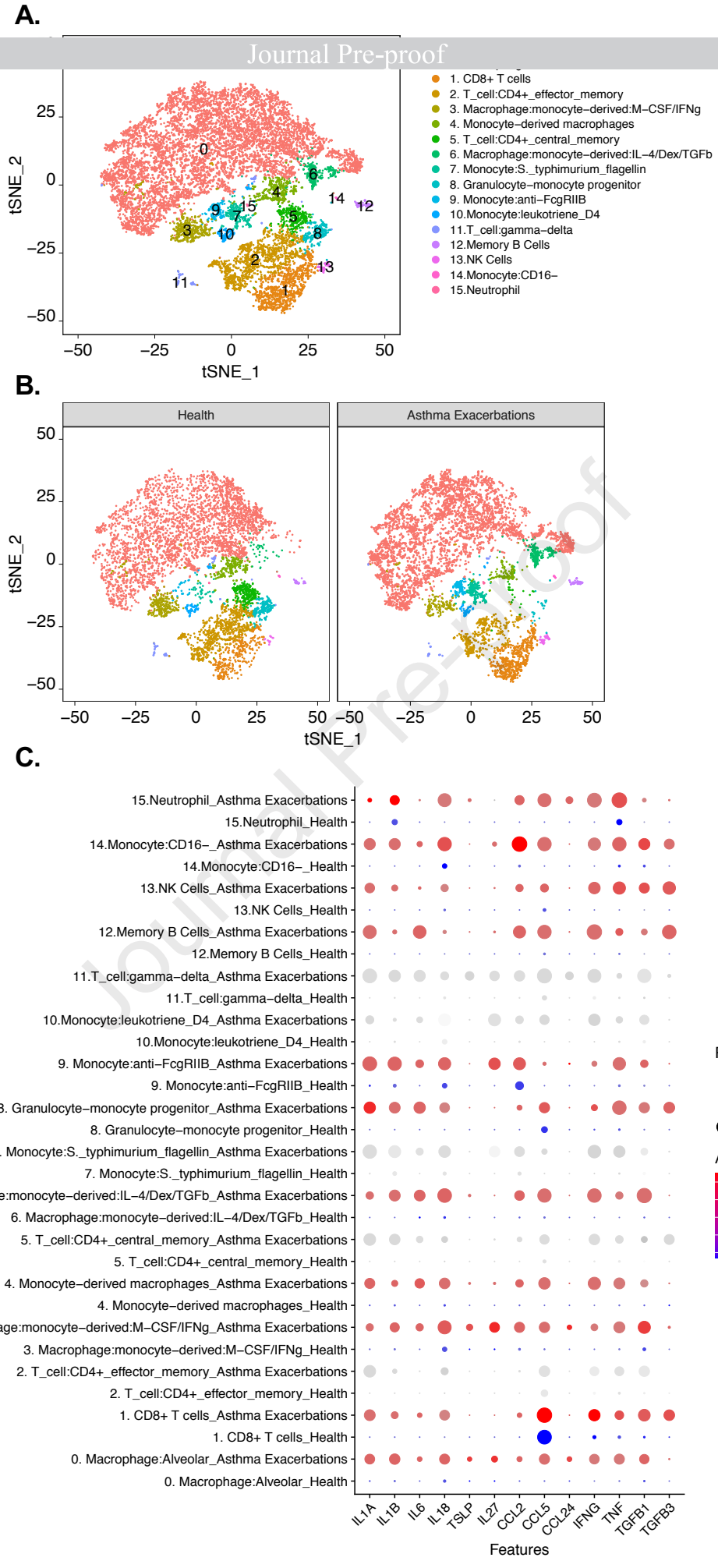


Fig 2.

Journal Pre-proof

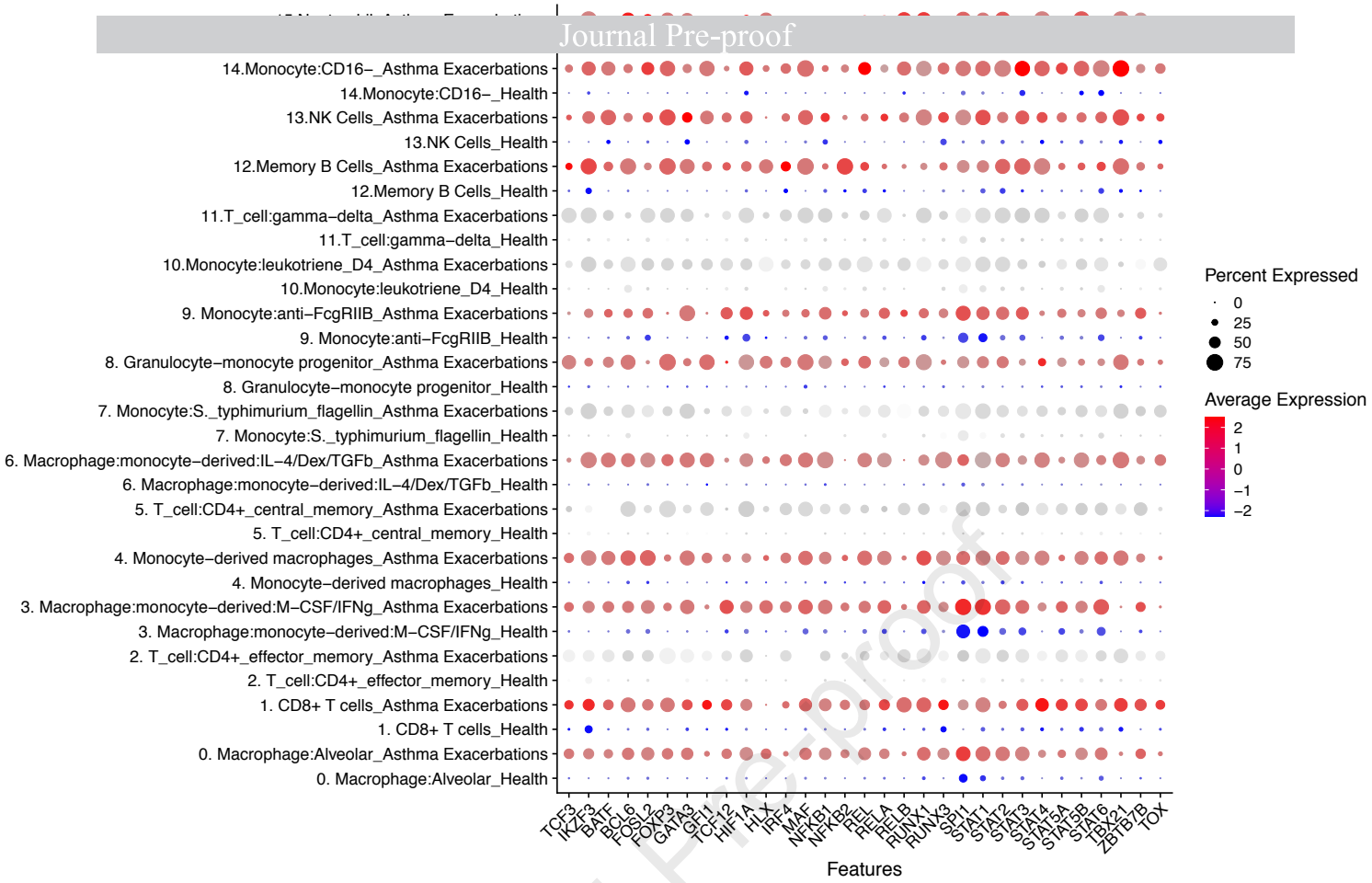
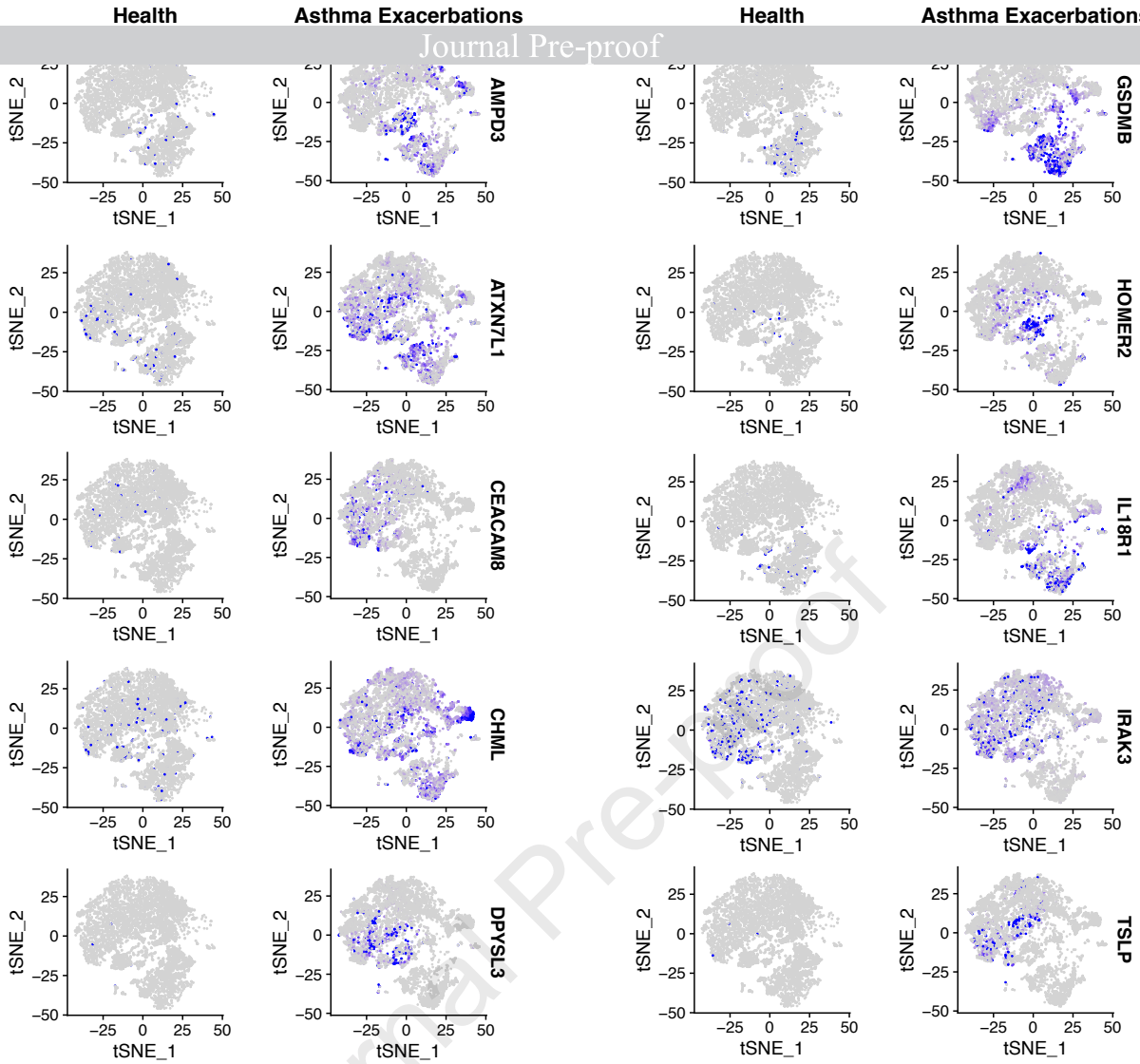


Fig 3.

Journal Pre-proof



Journal Pre-proof

Fig 4.

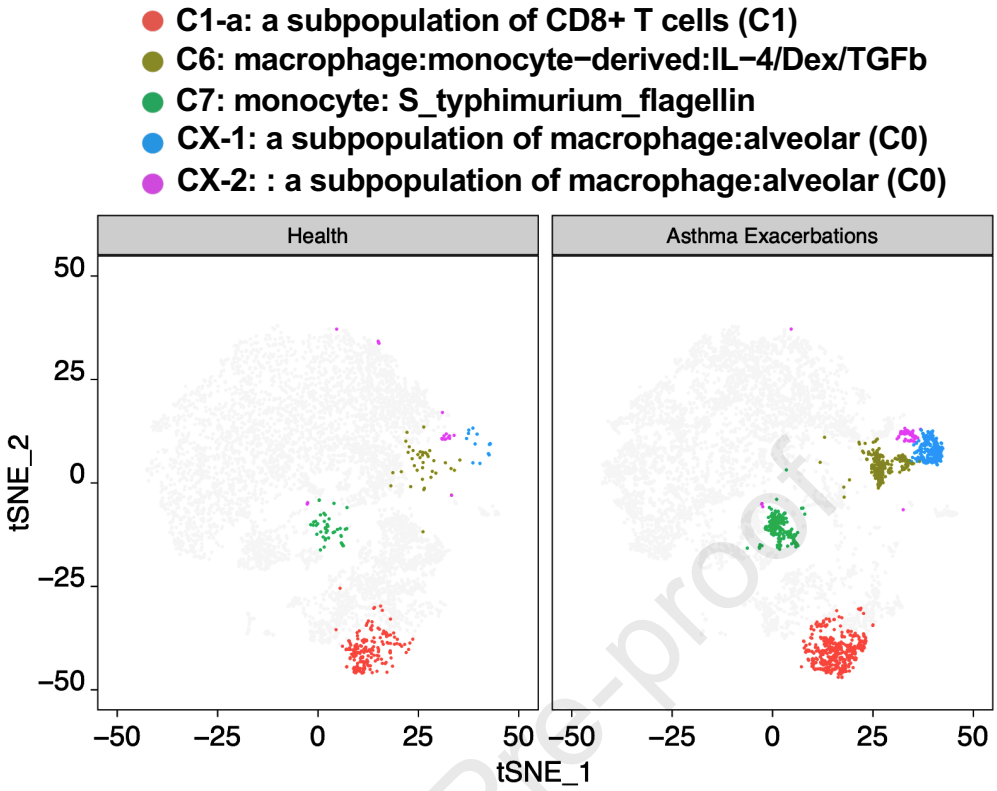
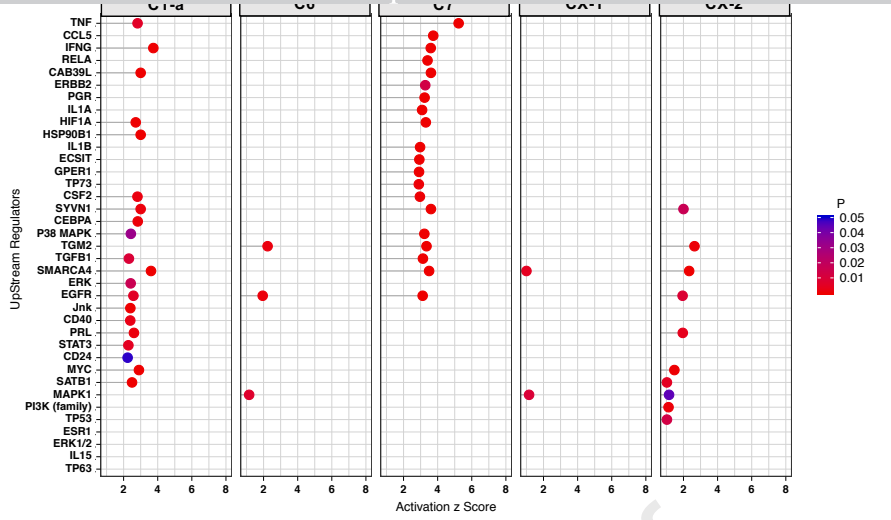


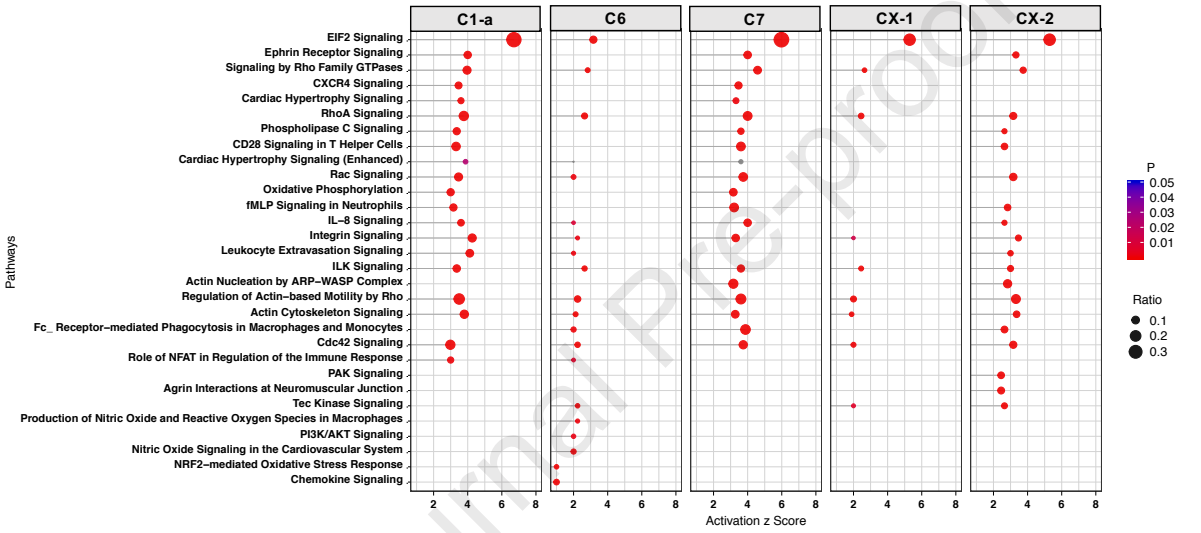
Fig 5.

Journal Pre-proof

Journal Pre-proof



B.



C.

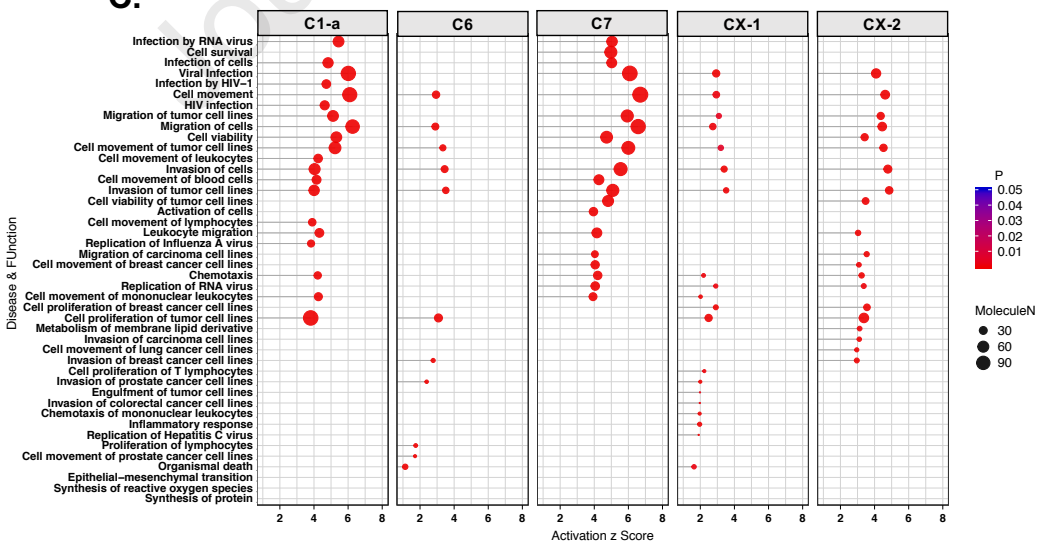


Fig 6.



Figure E1. t-SNE clustering by reference annotation. t-SNE map of immune cells in BALF of patients with asthma exacerbations, annotated with SingleR.